



**HAL**  
open science

## Age-dependent impact of streptozotocin on metabolic endpoints and Alzheimer's disease pathologies in 3xTg-AD mice

Geoffrey Canet, Maud Gratuze, Charleine Zussy, Mohamed Lala Bouali, Sofia Diego Diaz, Emma Rocaboy, Francis Laliberté, Noura B El Khoury, Cyntia Tremblay, Françoise Morin, et al.

### ► To cite this version:

Geoffrey Canet, Maud Gratuze, Charleine Zussy, Mohamed Lala Bouali, Sofia Diego Diaz, et al.. Age-dependent impact of streptozotocin on metabolic endpoints and Alzheimer's disease pathologies in 3xTg-AD mice. *Neurobiology of Disease*, In press, pp.106526. 10.1016/j.nbd.2024.106526 . hal-04587597

**HAL Id: hal-04587597**

**<https://hal.science/hal-04587597>**

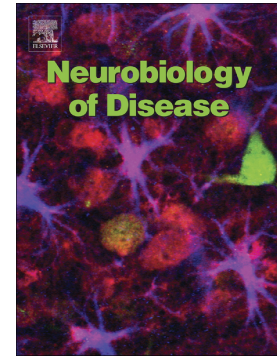
Submitted on 24 May 2024

**HAL** is a multi-disciplinary open access archive for the deposit and dissemination of scientific research documents, whether they are published or not. The documents may come from teaching and research institutions in France or abroad, or from public or private research centers.

L'archive ouverte pluridisciplinaire **HAL**, est destinée au dépôt et à la diffusion de documents scientifiques de niveau recherche, publiés ou non, émanant des établissements d'enseignement et de recherche français ou étrangers, des laboratoires publics ou privés.

Age-dependent impact of streptozotocin on metabolic endpoints and Alzheimer's disease pathologies in 3xTg-AD mice

Geoffrey Canet, Maud Gratuze, Charleine Zussy, Mohamed Lala Bouali, Sofia Diego Diaz, Emma Rocaboy, Francis Laliberté, Noura B. El Khoury, Cyntia Tremblay, Françoise Morin, Frédéric Calon, Sébastien S. Hébert, Carl Julien, Emmanuel Planel



PII: S0969-9961(24)00125-6

DOI: <https://doi.org/10.1016/j.nbd.2024.106526>

Reference: YNBDI 106526

To appear in: *Neurobiology of Disease*

Received date: 26 March 2024

Revised date: 6 May 2024

Accepted date: 7 May 2024

Please cite this article as: G. Canet, M. Gratuze, C. Zussy, et al., Age-dependent impact of streptozotocin on metabolic endpoints and Alzheimer's disease pathologies in 3xTg-AD mice, *Neurobiology of Disease* (2023), <https://doi.org/10.1016/j.nbd.2024.106526>

This is a PDF file of an article that has undergone enhancements after acceptance, such as the addition of a cover page and metadata, and formatting for readability, but it is not yet the definitive version of record. This version will undergo additional copyediting, typesetting and review before it is published in its final form, but we are providing this version to give early visibility of the article. Please note that, during the production process, errors may be discovered which could affect the content, and all legal disclaimers that apply to the journal pertain.

**Age-dependent impact of streptozotocin on metabolic endpoints and Alzheimer's disease pathologies in 3xTg-AD mice**

Running title: Age-dependent impact of streptozotocin in 3xTg-AD mice

**Geoffrey Canet<sup>1,2</sup>, Maud Gratuze<sup>1,3</sup>, Charleine Zussy<sup>1,2</sup>, Mohamed Lala Bouali<sup>1</sup>, Sofia Diego Diaz<sup>1</sup>, Emma Rocaboy<sup>1</sup>, Francis Laliberté<sup>2</sup>, Noura B. El Khoury<sup>1,4</sup>, Cyntia Tremblay<sup>2</sup>, Françoise Morin<sup>2</sup>, Frédéric Calon<sup>2,5</sup>, Sébastien S. Hébert<sup>1,2</sup>, Carl Julien<sup>6,7\*</sup>, Emmanuel Planel<sup>1,2\*</sup>**

<sup>1</sup> Laval University, Faculty of Medicine, Neurosciences and Psychiatry department, Québec, QC, G1V 0A6, Canada

<sup>2</sup> Neurosciences axis, CHU de Québec Research Center, Québec, QC, G1V 4G2 Canada

<sup>3</sup> Institute of Neurophysiopathology (INP), University of Aix-Marseille, CNRS UMR 7051, 13385 Marseille, France

<sup>4</sup> University of Balamand, Faculty of Arts and Sciences, Departement of Psychology, Tueini Building Kalhat, Al-Kurah, P.O. Box 100, Tripoli, Lebanon

<sup>5</sup> Laval University, Faculty of Pharmacy, Neurosciences and Psychiatry department, Québec, QC, G1V 0A6, Canada

<sup>6</sup> Research Center in Animal Sciences of Deschambault, Québec, QC, G0A 1S0, Canada

<sup>7</sup> Laval University, Faculty of Agricultural and Food Sciences, Québec, QC, G1V 0A6 Canada

Authors e-mail addresses: geoffrey.canet@crchudequebec.ulaval.ca; maud.gratuze@univ-amu.fr; charleine.zussy@umontpellier.fr; mohamed.lala-bouali@crchudequebec.ulaval.ca; sofia.diego-diaz.1@ulaval.ca; emma.rocaboy.1@ulaval.ca; cyntia.tremblay@crchul.ulaval.ca; noura.khoury@balamand.edu.lb; Françoise.Morin@crchudequebec.ulaval.ca; frederic.calon@crchudequebec.ulaval.ca; sebastien.hebert@crchudequebec.ulaval.ca; carl.julien@crsad.qc.ca; emmanuel.planel@neurosciences.ulaval.ca

**\*Correspondence should be addressed to:**

Dr. Carl Julien

CRSAD, 120-A chemin du Roy, Deschambault, QC, G0A 1S0, Canada

Tel: +1 (418) 286-3353 Fax: +1 (418) 286-3597

E-mail: carl.julien@crsad.qc.ca

or

Dr. Emmanuel Planel

CHUL P-9800, 2705 boulevard Laurier, Québec, QC, G1V4G2, Canada

Tel: +1 (418) 525-4444 (Ext: 47805) Fax: +1 (418) 654-2753

E-mail: emmanuel.planel@neurosciences.ulaval.ca

## ABSTRACT

Alzheimer's disease (AD) is a multifactorial neurodegenerative disease with a complex origin, thought to involve a combination of genetic, biological and environmental factors. Insulin dysfunction has emerged as a potential factor contributing to AD pathogenesis, particularly in individuals with diabetes, and among those with insulin deficiency or undergoing insulin therapy. The intraperitoneal administration of streptozotocin (STZ) is a widely used rodent model to explore the impact of insulin deficiency on AD pathology, although prior research predominantly focused on young animals, with no comparative analysis across different age groups. Our study aimed to fill this gap by analyzing the impact of insulin dysfunction in 7 and 23 months 3xTg-AD mice, that exhibit both amyloid and tau pathologies. Our objective was to elucidate the age-specific consequences of insulin deficiency on AD pathology.

STZ administration led to insulin deficiency in the younger mice, resulting in an increase in cortical amyloid- $\beta$  (A $\beta$ ) and tau aggregation, while tau phosphorylation was not significantly affected. Conversely, older mice displayed an unexpected resilience to the peripheral metabolic impact of STZ, while exhibiting an increase in both tau phosphorylation and aggregation without significantly affecting amyloid pathology. These changes were paralleled with alterations in signaling pathways involving tau kinases and phosphatases. Several markers of blood-brain barrier (BBB) integrity declined with age in 3xTg-AD mice, which might facilitate a direct neurotoxic effect of STZ in older mice.

Overall, our research confirms the influence of insulin signaling dysfunction on AD pathology, but also advises careful interpretation of data related to STZ-induced effects in older animals.

**Key words:** Alzheimer's disease, Insulin deficiency, diabetes mellitus, Streptozotocin, tau phosphorylation, amyloid- $\beta$ , blood-brain-barrier, 3xTg-AD mice.

## INTRODUCTION

Alzheimer's disease (AD) is the predominant cause of dementia worldwide, and is characterized by two main pathological features in the brain: senile plaques, composed of extracellular deposits of amyloid-beta ( $A\beta$ ) peptides, and intraneuronal neurofibrillary tangles containing hyperphosphorylated tau (Long and Holtzman, 2019; Korczyn and Grinberg, 2024). The vast majority of AD cases (~99%) manifest as late-onset and sporadic, with various genetic, biological and environmental factors contributing to its etiology (Querfurth and LaFerla, 2010; Korczyn and Grinberg, 2024).

Among these factors, there is increasing evidence suggesting that either insulin resistance or insulin deficiency represents important risk factors for sporadic AD (Rönnemaa et al., 2008; Pugazhenthii et al., 2017; Rhea et al., 2023; Yoon et al., 2023). Epidemiological data demonstrate a higher risk of AD in patients with type-2 diabetes mellitus (T2DM), especially those in the advanced stages of insulin deficiency requiring insulin therapy (Ott et al., 1999; Sims-Robinson et al., 2010). Due to recent advances in diabetes management, individuals diagnosed with type-1 diabetes (T1DM) are experiencing increased longevity, but face elevated risk of dementia (Whitmer et al., 2021). Several studies have also revealed cerebral anomalies in the central levels of insulin, impaired insulin receptor expressions and localization, along with reduced glucose metabolism in AD patients brain (Frölich et al., 1999; Ott et al., 1999; Craft and Stennis Watson, 2004; Sims-Robinson et al., 2010; Gratuze et al., 2019; Leclerc et al., 2023). Overall, both central and peripheral insulin dysfunction emerge as potential risk factors in AD (Rönnemaa et al., 2008; Pugazhenthii et al., 2017; Yoon et al., 2023).

The intraperitoneal administration of streptozotocin (STZ) in rodent models has been extensively utilized to study the influence of peripheral insulin deficiency on AD pathology. Despite the fact that AD is an age-related disorder, prior research predominantly focuses on younger animals, with no comparative analysis spanning different age cohorts. Our study sought to bridge this gap by assessing the influence of insulin dysfunction in both middle-aged and old 3xTg-AD mice, aged 7 and 23 months, respectively. Our objective was to dissect the age-specific effects of insulin signaling impairments on AD pathology, reflecting the insulin deficiency observed in T1DM and late-stage T2DM patients (Barbagallo and Dominguez, 2014; Whitmer et al., 2021).

Our findings indicate that STZ administration in younger mice induced peripheral insulin deficiency, and promoted A $\beta$  burden and insoluble tau aggregation, yet did not affect tau phosphorylation. In contrast, STZ administration in older mice, despite causing no observable circulating insulin deficiency, induced tau hyperphosphorylation and aggregation with no A $\beta$  accumulation. These alterations were accompanied by changes in signaling pathways involving tau kinases and phosphatases. As 3xTg-AD mice aged, several indicators of blood-brain barrier (BBB) integrity decreased, potentially facilitating a direct neurotoxic effect of STZ in older mice. In summary, our findings reinforce the significance of insulin signaling dysfunction in AD pathology and underscore the need for careful interpretation of STZ-induced effects in aged animal models.

## RESEARCH DESIGN & METHODS

### Animals

The experimental procedures involving the mice were carried out in accordance with the guidelines provided by the Canadian Council on Animal Care and were approved by the "The Animal Care Committee of Université Laval" (CPAUL-3, approval number: CHU-22-1027)". Male 3xTg-AD mice, aged 7 and 23-months, were used in this study. We decided to not include wild-type control mice in our study because the purpose of the present study was to evaluate the effects of STZ in the context of AD-like pathology, which is not present in non-transgenic mice. Moreover, the impact of STZ administration in wild-type mice has already been extensively documented in literature by us and others (Clodfelder-Miller et al., 2006; Planel et al., 2007b; Jolivald et al., 2008; Kim et al., 2009; Ding et al., 2021). 3xTg-AD mice carry three distinct mutant genes: amyloid- $\beta$  protein precursor (A $\beta$ PP<sub>swe</sub>), presenilin-1 (PS1M146 V), and tau (P301L). The mice were derived from a colony maintained within our animal facilities and were originally obtained from Dr. Frank LaFerla's laboratory (Oddo et al., 2003; Billings et al., 2005). This mouse model exhibits AD hallmarks, including plaque and tangle pathologies. The animals were housed in a controlled environment at a temperature of 22°C, with a 12-hour light and 12-hour dark cycle. Food and water were provided to the animals ad libitum.

### Streptozotocin injections

Nonfasted animals were subjected to the Multiple Low-Dose STZ induction protocol as outlined by the "Animal Models for Diabetic Complications Consortium" (Hsueh et al., 2007). This protocol involved the administration of a daily intraperitoneal injection of 50 mg/kg of STZ (Sigma, St. Louis, MO) for a duration of five consecutive days. STZ was freshly dissolved in a vehicle solution consisting of 0.05 M citrate buffer at pH 4.5. This approach offers the advantage of inducing a long-lasting insulin deficiency condition in the mice, with minimal toxicity. Vehicle-injected mice served as controls.

### Physiological parameters monitoring

The diagnosis of insulin deficiency was established through the monitoring of several physiological parameters in the mice. Glycosuria was assessed using urinalysis reagent strips (Diastix; Bayer HealthCare, Pittsburgh, PA). Nonfasting blood glucose levels were determined with a glucometer equipped with reagent strips (ACCU-CHEK Aviva Nano; Roche Diagnostics,

Mannheim, Germany) or a Glucose Assay Kit (Biovision Inc., Mountain View, CA). Plasma insulin concentrations were quantified using a sandwich enzyme immunoassay following the manufacturer's instructions (Mouse Insulin ELISA, Mercodia, Sweden). At the time of sacrifice, all mice were weighed, and their body temperature was monitored using a rectal probe (Thermalert TH-5; Physitemp, Clifton, NJ).

### **Preparation of Mouse Brain Protein Extracts**

At three months ( $14 \pm 1$  weeks) following STZ injections, mice were euthanized by decapitation without anesthesia, as the use of anesthesia has been shown to increase hypothermia-induced tau phosphorylation (Planel et al., 2007a; Canet et al., 2023). The brains were promptly removed and dissected on ice. Tissue samples were immediately frozen on dry ice and stored at  $-80^{\circ}\text{C}$ . Protein extracts from the cerebral cortices were prepared through homogenization (PowerGen 125, Fisher Scientific, Ottawa, ON, Canada) in a RIPA buffer containing 50 mM Tris-HCl at pH 7.4, 1 mM EDTA, 150 mM NaCl, 0.5% sodium deoxycholate, 1% NP-40, along with phosphatase inhibitors (1 mM sodium vanadate and 1 mM sodium fluoride) and protease inhibitors (Protease Inhibitors Cocktail P8340, Sigma-Aldrich, at 10  $\mu\text{l/ml}$ , and 1 mM PMSF). The resulting homogenates were then centrifuged at 20,000 x g for 20 minutes at  $4^{\circ}\text{C}$ , after which the supernatants were collected and stored at  $-80^{\circ}\text{C}$ .

### **Analysis of tau solubility**

The solubility of tau was assessed with a modification of the protocol initially described by Greenberg and Davies (Greenberg and Davies, 1990; Canet et al., 2024). In brief, 100  $\mu\text{l}$  of the supernatant of protein extract (as previously detailed) was adjusted to a 1% Sarkosyl (N-lauroylsarcosine) concentration. This mixture was incubated for 1 hour at room temperature with continuous agitation and subsequently centrifuged at 100,000 x g for 1 hour at  $20^{\circ}\text{C}$ . The resulting pellet, which contains Sarkosyl-insoluble aggregated tau, was resuspended and then subjected to Western blot analysis. The tau presents in the Sarkosyl-insoluble fraction has been demonstrated to exhibit filamentous characteristics, a hallmark feature of tau in NFTs (Noble et al., 2003).

### **Western Blot Analysis**

Western blot analysis was performed according to our established protocols (Fereydouni-Forouzandeh et al., 2024). Samples containing 10-20  $\mu\text{g}$  of protein were separated on a 10%

SDS-polyacrylamide gel and subsequently transferred onto nitrocellulose membranes (Amersham Biosciences). The membranes were then blocked, probed with the relevant antibodies, and revealed following the methodology described in (Fereydouni-Forouzandeh et al., 2024). Details regarding the antibodies used, as well as their respective dilutions, can be found in Table 1. In the case of immunoblots targeting phosphorylated tau epitopes, the signal intensity was normalized to total tau protein. Other proteins were normalized to  $\beta$ -actin levels. Representative lanes from the immunoblots were displayed for each specific experimental condition. The dashed lines indicate segments where certain lanes from the same blot were excluded, and the remaining lanes were combined. Brightness levels were adjusted as necessary to enhance visualization and accuracy.

### **Biochemical assessment of A $\beta$ pathology**

Soluble and insoluble A $\beta$ 40 and A $\beta$ 42 were assayed by ELISA kits (Wako, Osaka, Japan) as described in (Julien et al., 2010) with slight modifications. In brief, frozen mouse cortical tissues were sonicated in tris-buffered saline (TBS) supplemented with protease and phosphatase inhibitors. Subsequently, the samples were centrifuged at  $100,000 \times g$  for 20 minutes at  $4^{\circ}\text{C}$  to obtain a TBS-soluble fraction, containing intracellular and extracellular A $\beta$  species. The TBS-insoluble pellet was sonicated in RIPA buffer supplemented with protease and phosphatase inhibitors, and then centrifuged at  $100,000 \times g$  for 20 minutes at  $4^{\circ}\text{C}$ . The resulting pellets were homogenized in 100  $\mu\text{l}$  of 98% formic acid with a brief sonication ( $3 \times 10$  seconds). The resulting suspension was subjected to centrifugation at  $15,000 \times g$  for 20 minutes at  $4^{\circ}\text{C}$ , after which the supernatant was dried at room temperature and solubilized in guanidine buffer (containing 5M guanidine/50 mM Tris-HCl at pH 8.0) (insoluble fraction). Soluble A $\beta$ 40 and A $\beta$ 42 levels were quantified using the Human  $\beta$  Amyloid (1–42) ELISA kit from WAKO, High Sensitive (WAKO, Osaka, Japan). Both ELISA assays were conducted according to the manufacturer's recommendations, and the plates were read at 450 nm using a Synergy HT multi-detection microplate reader (Biotek, Winooski, VT).

### **Statistical Analysis**

Prior to conducting each analysis of variance, an assessment of Gaussian distribution was performed, and its validity was confirmed through a Kolmogorov-Smirnov test (utilizing GraphPad Prism 9.0). Depending on the specific analysis, two-tailed t-tests or two-way ANOVAs were applied. Post hoc analyses, involving either Tukey's tests, were subsequently employed. A

significance threshold of  $P < 0.05$  was determined. All data are reported as mean  $\pm$  SD. The scatter plots depicted on each graph provide an indication of the number of data points, and detailed statistical information is provided in Supplementary Table 1.

Journal Pre-proof

## RESULTS

### **Streptozotocin (STZ) treatment elicits age-dependent tau hyperphosphorylation and aggregation in 3xTg-AD mice**

To investigate insulin dysfunction in a murine model exhibiting both A $\beta$  and tau pathologies, we administered STZ to 7- and 23-month-old 3xTg-AD mice (Fig. 1a), aiming to induce a model of insulin deficiency (Ganda et al., 1976). As anticipated, a daily dose of 50 mg/kg STZ over 5 consecutive days led to immediate hyperglycemia and glycosuria (Fig. 1b-e), as well as a significant reduction in insulinemia (Fig. 1f), in 7-month-old 3xTg-AD mice. Intriguingly, the 23-month-old 3xTg-AD mice injected with STZ displayed no significant decrease in insulinemia, a delayed hyperglycemic response, with a peak between 30 and 45 days that returned to near control levels at the time of euthanasia, and only 20% of the mice displayed glycosuria (Fig. 1b-e). These results suggest that STZ had limited effects on diabetic markers in the older mice. However, both young and old animals exhibit a significant body weight loss following STZ administration (Fig. 1g), a characteristic feature of insulin deficiency. Given the low incidence of insulin deficiency-related symptoms in the older 3xTg-AD mice following STZ injection, and to enhance the reliability of our analyses, we excluded the two mice with glycosuria and a mouse that displayed profound hypothermia (31.2°C).

Subsequently, we used western blot analysis to assess whether STZ induced alterations in tau phosphorylation in the cortices of 7- and 23-month-old 3xTg-AD mice. The cortical phosphorylation level of tau was assessed using specific antibodies targeting phosphorylated tau at distinct epitopes, including AT8 (pS202/pT205) (Mercken et al., 1992; Goedert et al., 1995), PHF1 (pS396/pS404) (Otvos et al., 1994), AT180 (pT231/pS235) (Goedert et al., 1994), Tau-1 (tau dephosphorylated at S195/S198/S199/S202) (Szendrei et al., 1993), AT270 (pThr181) (Goedert et al., 1994), CP13 (pSer202) (Weaver, 2000), MC6 (pSer235) (Jicha et al., 1997), pS199, pS404, pS422, TG3 (pT231) (Jicha et al., 1997), and 12E8 ('KXGS' motifs at pS262, pS356) (Seubert et al., 1995). These particular tau antibodies were chosen due to their relevance to AD-related pathological processes, such as pretangle formation (AT8, CP13), paired helical filament and NFT formation (AT8, CP13, MC6, PHF1) (Goedert et al., 1994; Augustinack et al., 2002), as well as the disruption of tau binding to microtubules (12E8) (Litersky et al., 1996). All other phosphoepitopes were found to exhibit abnormal phosphorylation patterns in the AD brain (Šimić et al., 2016). Therefore, these antibodies were deemed appropriate for providing a

comprehensive assessment of the impact of insulin dysfunction on tau phosphorylation. While 7-month-old 3xTg-AD mice did not exhibit changes in tau phosphorylation (Fig. 2), STZ treatment resulted in a significant increase in tau phosphorylation at the AT8, AT180, TG3, MC6 and 12E8 epitopes, along with notable trend at AT270 (+76%,  $p=0.06$ ) in the 23-month-old 3xTg-AD mice compared to the non-treated control group (Fig. 2). The levels of total tau (TauC, C-terminal residue of tau) remained unchanged between groups (Fig. 2m).

The presence of insoluble tau aggregates is a pathological hallmark of AD (Long and Holtzman, 2019), and tau hyperphosphorylation is believed to be implicated in this detrimental process (Trojanowski and Lee, 1994; Alonso et al., 1996). We observed a significant increase in tau aggregation, as measured by sarkosyl-insoluble tau, in both young and old 3xTg-AD mice following STZ administration (Fig. 2n). Collectively, these findings demonstrate that STZ induces tau hyperphosphorylation and aggregation more prominently in 23-month-old 3xTg-AD mice.

#### **Impact of STZ treatment on tau kinases**

Given the stronger impact of STZ on tau phosphorylation and aggregation in the cortices of 23-month-old 3xTg-AD mice, we examined the activities of specific tau kinases commonly involved in tau hyperphosphorylation including GSK3- $\beta$  (glycogen synthase kinase 3- $\beta$ ), CDK5 (cyclin dependent kinase 5), and its activators p25/35, ERK (Extracellular signal-Regulated Kinase), JNK (c-Jun N-terminal Kinase), CAMKII (Ca<sup>2+</sup>/calmodulin-dependent protein Kinase II), and AKT (Protein B Kinase) (Planel et al., 2002; Martin et al., 2013b). STZ treatment significantly elevated the expression levels of p35 (Fig. 3k) and CDK5 (Fig. 3l), while the levels of the other kinases did not change significantly compared to non-treated 23-month-old mice. It is noteworthy that CDK5 and its activator p25/35 can phosphorylate tau at the AT8, MC6, and TG3 epitopes (Planel et al., 2002; Martin et al., 2013b) that were hyperphosphorylated following STZ treatment (Fig. 2) Overall, these results suggest that CDK5 activation might have played a role in tau hyperphosphorylation at AT8, Tau-1, AT180 and MC6 induced by STZ in older 3xTg-AD mice. However, it failed to account for all the epitopes hyperphosphorylated.

#### **Effect of STZ treatment on tau phosphatases**

As CDK5 activation alone cannot explain the extent of tau hyperphosphorylation in old 3xTg-AD mice, we assessed the levels of the protein phosphatases PP1, PP2B, PP2A, and PP5. Tau

dephosphorylation processes are primarily supported by PP2A (Martin et al., 2013a), although PP1, PP2B, and PP5 can also contribute to these processes. PP2A is a heterotrimer composed of a scaffolding A subunit, a catalytic C subunit, and a regulatory B subunit (Hoffman et al., 2017). Immunoblot analysis revealed a global decrease in PP2A activation, as indicated by the elevated expression of the demethylated form of PP2AC (Fig. 4e). STZ injections in 23-month-old 3xTg-AD mice also resulted in increased expression levels of the PP2A-B $\beta$  regulatory subunit (Fig. 4d), total PP2AC (Fig. 4f), and PP2B (Fig. 4g). No changes were observed in PP1, PP2A-A, PP2A-B $\alpha$  subunit, or PP5 levels in the cortices of STZ-treated mice compared to controls (Fig. 4a,b,c,h). In summary, these results suggest that STZ-induced tau hyperphosphorylation in 3xTg-AD mice may involve the deregulation of PP2A and PP2B activities.

### **Effect of STZ treatment on A $\beta$ pathology in 3xTg-AD**

We subsequently assessed the impact of STZ on A $\beta$  production and accumulation in 7- and 23-month-old 3xTg-AD mice. ELISA assays revealed an age-dependent increase in both soluble and insoluble A $\beta$  levels (Fig. 5). Administration of STZ in 7-months old 3xTg-AD mice resulted in a reduction in the levels of insoluble A $\beta$ 40 (Fig. 5d), leading to an alteration in the A $\beta$ 42/A $\beta$ 40 ratio (Fig. 5f), favoring the more toxic A $\beta$ 42 isoform. Moreover, there was a discernible trend ( $p = 0.08$ ) toward increased level of soluble A $\beta$ 42 in young mice following STZ treatment (Fig. 5b). STZ treatment in young and old 3xTg-AD mice also increased the expression of the C99 fragment of APP (Fig. 5h), despite total APP and  $\beta$ -site APP cleaving enzyme 1 (BACE1) levels remained unchanged (Fig. 5g,i). Nonetheless, under our experimental conditions, it did not seem that STZ administration exacerbated the already elevated A $\beta$  burden in aged 3xTg-AD mice.

### **Effect of STZ treatment on synaptic markers in 3xTg-AD**

In a previous study, we identified that a high-fat diet led to a reduction in drebrin expression in 3xTg-AD mice, suggesting an exacerbation of synaptic deficits (Julien et al., 2010). To assess whether STZ treatment aggravated synaptic deficits in 3xTg-AD mice, we analyzed synaptic markers in 7- and 23-month-old animals. Immunoblot analysis revealed an age-dependent decline in drebrin and synaptophysin expressions (Fig. 6a, c). Notably, a trend toward reduced drebrin ( $p = 0.10$ ) and synaptophysin expressions were observed following STZ administration in young 3xTg-AD mice (Fig. 6a, c). Surprisingly, we also observed an increase in synaptophysin levels (Fig. 6c) in 23-month-old mice following STZ treatment. However, we did not find any changes in the levels of post-synaptic density protein 95 (PSD-95) or synaptosomal-associated protein-25

(SNAP-25) (Fig. 6b,d). Collectively, these results demonstrate that STZ treatment did not induced notable synaptic deficits in the 3xTg-AD mouse model.

### **Effect of STZ treatment on brain insulin receptor in 3xTg-AD**

We further evaluated the impact of STZ on brain insulin receptor by analyzing the ratio of phospho-insulin receptor (IR) to total IR level and the phosphatidylinositide 3-kinase (PI3K)/AKT signaling pathway in the cortex of 7- and 23-month-old 3xTg-AD mice. Immunoblot analysis revealed an increase in the expression ratio of pIR/IR (Fig. 7a) and elevated PI3K levels (Fig. 7d) in 7-month-old STZ-treated mice. We also noticed an age-dependent decrease in the activity of PI3K (Fig. 7c), as well as in the expression of insulin degrading enzyme (IDE) (Fig. 7e) between 7- and 23-months old 3xTg-AD mice. These observations suggest an age-dependent resistance to STZ effect in 3xTg-AD mice.

### **Effect of STZ treatment on blood-brain barrier (BBB) markers**

STZ's similarity to glucose enables it to enter cells *via* the glucose transport protein GLUT2, which explains its toxicity to pancreatic  $\beta$  cells, since they express high levels of GLUT2 (Schneidl et al., 1994). The expression of GLUT2 in the brain is limited to specific regions (Koepsell, 2020), and it is generally admitted that STZ does not cross the BBB (Grieb, 2016; Sweeney et al., 2019). However, a BBB breakdown occurs with aging in 3xTg-AD mice and older animals (Bourasset et al., 2009; Erdő et al., 2017), which could lead to a direct effect of STZ in the brain. This is important since ICV injections of STZ are known to promote AD pathology in laboratory animals (Grieb, 2016).

To investigate whether tau hyperphosphorylation might be attributed to BBB dysfunction facilitating a direct effect of STZ on the brain, we analyzed proteins of tight junctions and adherence junctions involved in maintaining BBB integrity (Sweeney et al., 2019). We observed an age-dependent reduction in the expression levels of these proteins, as Zonula Occludens-1 (ZO1) (Fig. 8a), occludin (Fig. 8b), and vascular endothelial (VE)-cadherin (Fig. 8c) in 23-month-old mice compared to 7-month-old controls. Additionally, STZ treatment induced a decrease in occludin expression in young 3xTg-AD mice (Fig. 8b). These findings confirm the age-dependent breakdown of the BBB in aged 3xTg-AD mice and suggest that STZ might have infiltrated the brain, potentially eliciting direct effects in older animals.

## DISCUSSION

In this study, we assessed the age-dependent impact of STZ-induced insulin deficiency on AD-like pathology in 3xTg-AD mice. In 7-month-old 3xTg-AD mice, STZ treatment led to hyperglycemia and insulin deficiency, resulting in A $\beta$  and tau accumulation without tau hyperphosphorylation. In contrast, 23-month-old 3xTg-AD mice were resilient to the peripheral metabolic impact of STZ, while displaying increased tau phosphorylation and aggregation, but no change in A $\beta$ . These age-related discrepancies and their implications for AD are discussed below.

We first validated the induction of insulin deficiency in 7- and 23-month-old 3xTg-AD mice and observed an age-dependent response to STZ. The 7-month-old 3xTg-AD mice injected with STZ exhibited immediate hyperglycemia, hypo-insulinemia and glycosuria. In contrast, the STZ-treated 23-month-old animals had delayed and transient hyperglycemia, no change in insulinemia and inconsistent glycosuria. These results are consistent with prior observations demonstrating that the hyperglycemic effect of STZ is markedly reduced and transient in older mice, potentially due to either a higher vulnerability of  $\beta$  cells in younger mice or to age-related changes in STZ pharmacokinetics, and to  $\beta$  cells regeneration in older mice (Riley et al., 1981). In addition, 3xTg-AD tend to exhibit some T2DM features with aging, such as altered glycemic responses and a global reduction in pancreatic islet volume (Vandal et al., 2015; Griffith et al., 2019), which might have further impacted the efficacy of STZ. Collectively, these findings imply that STZ had its full intended effect in the 7-month-old 3xTg-AD mice, while the 23-month-old 3xTg-AD mice were partly resistant to the effects of the drug.

We next conducted a thorough examination of tau phosphorylation in the same mice. Although STZ failed to induce diabetes in the 23-month-old 3xTg-AD mice, it elicited substantial hyperphosphorylation of tau at multiple epitopes. Conversely, no significant alterations were detected in the 7-month-old 3xTg-AD mice, even in the presence of features indicative of insulin deficiency. These conflicting results led us to hypothesize that STZ might have exerted a direct effect on the brain in the 23-month-old 3xTg-AD mice. Supporting this hypothesis, intracerebroventricular injections of STZ have been shown to induce both brain insulin signaling dysfunction (Grünblatt et al., 2007; Plaschke et al., 2010) and tau hyperphosphorylation (Chen et al., 2014) in 3xTg-AD mice. However, STZ is transported by GLUT2, which is only expressed in specific regions in the brain (Koepsell, 2020), and it is generally considered that it cannot

normally cross the BBB (Schredl et al., 1994). Nevertheless, previous research, including our own findings (Bourasset et al., 2009), have indicated a compromised BBB in aged 3xTg-AD mice (Mehta et al., 2013; Do et al., 2014; Islas-Hernandez and Garcia-Delatorre, 2020). We further confirmed here that many markers of BBB integrity were decreased in the 23-month-old 3xTg-AD mice. Hence, the pronounced effect of STZ treatment on tau pathology in older 3xTg-AD mice might be attributed to a higher brain bioavailability of STZ. It is also important to mention that a compound does not necessarily have to cross the BBB to exert neurotoxicity/neuroprotection, especially when impacting metabolic function (Leclerc et al., 2021).

We were surprised by the absence of tau hyperphosphorylation in the young mice despite the induction of diabetes by STZ. Indeed, our meta-analytical examination (Table 2) of various studies utilizing STZ i.p. injections to induce insulin deficiency consistently reported tau hyperphosphorylation in young wild-type and AD mouse models, including 3xTg-AD (Imamura et al., 2020; Wang et al., 2020), pR5 (Ke et al., 2009), and h-APP (Jolivalt et al., 2010). Discrepancies in findings across studies may be attributable to variations in experimental protocols, particularly the use of anesthesia prior to euthanasia (Table 2), which is known to cause hypothermia-induced tau hyperphosphorylation (Planel et al., 2007a, 2009; Canet et al., 2023). This effect is particularly pertinent in rodent models of diabetes, both STZ-induced and genetic, which are known to exhibit thermoregulatory impairments and BT daily rhythms alterations (Trayhurn, 1979; Ramos-Lobo et al., 2015), possibly exacerbating the hypothermic response to anesthesia exposure. Other sources of discrepancies include the dose of STZ and the duration of the study. For instance, Wang *et al.* administered a higher dose of STZ to young 3xTg-AD mice and conducted tau analysis after 8 weeks, whereas our study extends the analysis to 3 months post-administration (Wang et al., 2020). Ke *et al.*, used a single high-dose injection (200 mg/kg) (Ke et al., 2009), which could induce side effects not observed with lower dosages, such as hypothermia and subsequent tau phosphorylation (Planel et al., 2007b). Nonetheless, some research also failed to evidence a marked tau hyperphosphorylation either in 12-months old 3xTg-AD mice (Hayashi-Park et al., 2017) or in young hTau mice (Trujillo-Estrada et al., 2019) following STZ administration. While our findings provide important evidence into the role of insulin dysfunction in mediating tau pathology, it is imperative to acknowledge the limitations inherent in animal models and pharmacological methods for modeling human diseases in rodents. This emphasizes the importance of standardizing STZ injections protocols, as outlined by the

“Animal Models for Diabetic Complications Consortium” (Hsueh et al., 2007),, as well as controlling animals’ core body temperature and avoiding the use of anesthesia, whenever feasible, to prevent tau phosphorylation artifacts (Canet et al., 2023).

In AD, the progressive aggregation and accumulation of tau correlates with memory impairments (Pollak et al., 2003; Long and Holtzman, 2019). Thus, we proceeded to investigate tau aggregation by isolating the sarkosyl-insoluble fraction (Greenberg and Davies, 1990). Our results revealed that STZ administration exacerbates tau aggregation to a greater extent in 23-month-old 3xTg-AD mice compared to their 7-month-old counterparts. While the results in the old mice were anticipated, the increase of insoluble tau levels in the young mice was perplexing, given that tau hyperphosphorylation is often considered to be a prerequisite for aggregation (Trojanowski and Lee, 1994; Alonso et al., 2001). Indeed, hyperphosphorylated tau can trigger aggregation *in vitro* (Alonso et al., 2001; Sato et al., 2002) and is believed to promote the formation of neurofibrillary tangles (Trojanowski and Lee, 1994). However, this hypothesis is challenged by some (Haj-Yahya et al., 2020; Wegmann et al., 2021), and it is worth noting that insoluble tau accumulation can occur without alterations in tau phosphorylation levels, as observed in studies investigating sleep deprivation in 3xTg-AD mice (Di Meco et al., 2014). These findings further extent our understanding of age-dependent STZ effects on tau pathology in 3xTg-AD mice.

Subsequently, we aimed to elucidate the mechanisms underlying tau hyperphosphorylation by analyzing the major tau kinases and phosphatases in STZ-treated 23-month-old 3xTg-AD mice. We focused on this age group as young animals did not exhibit any notable changes in tau phosphorylation. We observed an increase of CDK5 expression after STZ treatment, contrasting some prior findings that showed reduced CDK5 levels in T1DM models (Papon et al., 2013; Gratuze et al., 2017). Elevated expression of CDK5 might have played a role in the elevated phosphorylation of tau at S202, T205, T181 and T231, as it can phosphorylate these epitopes (Kimura et al., 2014). However, it was probably not sufficient to explain the extent of tau hyperphosphorylation. Such tau hyperphosphorylation likely pertains to decreased PP2A activity, as indicated by increased demethylation of its catalytic subunit. Notably, PP2A is the most effective regulator of tau protein phosphorylation, and even its partial inhibition can account for tau hyperphosphorylation across most of phospho-epitopes (Gong et al., 1993; Martin et al., 2013a). Inhibition of PP2A is further supported by the increase in the total levels of the catalytic

subunit of PP2A (PP2AC). Indeed, it was reported that PP2A inhibition leads to its catalytic subunit accumulation as a compensatory mechanism (Baharians and Schönthal, 1998; Planel et al., 2001). These findings substantiate the pivotal role of PP2A in tau hyperphosphorylation following STZ administration. Numerous studies have previously reported decreased PP2A expression associated with a decrease of its activity, in both spontaneous (Papon et al., 2013) and induced (Clodfelder-Miller et al., 2006; Planel et al., 2007b; Qu et al., 2011) insulin deficiency models, explaining tau hyperphosphorylation. Collectively, our results suggest that PP2A signaling may represent a crucial link between diabetes and AD, as dysregulation in PP2A activity is associated with tau hyperphosphorylation.

The effects of STZ-induced insulin deficiency on A $\beta$  burden remain a topic of debate. Prior research has demonstrated that insulin dysfunction can exacerbate A $\beta$  accumulation *in vivo* (Gasparini, 2002; Liu et al., 2008; Leclerc et al., 2023). Our findings in 7-month-old 3xTg-AD mice align with these observations as STZ injections led to an increased ratio of insoluble A $\beta$ <sub>42</sub>/A $\beta$ <sub>40</sub>, as well as C99 expression, which is relevant to AD pathology (Selkoe, 2001). Further investigations are needed to determine the mechanisms underlying the increase in A $\beta$  production and accumulation in young 3xTg-AD mice. Indeed, following STZ treatment, 7-months old 3xTg-AD mice exhibits some features related to insulin dysfunction and known to promote amyloid pathology such as chronic hyperglycemia (Macauley et al., 2015) and a reduced expression of IDE, the main enzyme involved in A $\beta$  degradation (Tanzi et al., 2004). In contrast, we did not observe any change in A $\beta$  in 23-month-old 3xTg-AD mice following STZ injections, similar to previous observations (Chen et al., 2014). This discrepancy may be attributed to the already high amyloid load in older 3xTg-AD mice, making it challenging to discern an exacerbation post-STZ treatment, despite the increase in C99 expression. The considerable variability in data from different studies investigating A $\beta$  in animals exposed to STZ underscores the debatable role of insulin deficiency in A $\beta$  burden. Further investigations are warranted to elucidate the impact of insulin deficiency on A $\beta$  pathology.

Synaptic dysfunction is a well-established feature exhibited by 3xTg-AD mice (Oddo et al., 2003), with the decrease of synaptic markers like SNAP-25 and PSD95 (Carvalho et al., 2015). We previously demonstrated that a high-fat diet decreases the level of postsynaptic drebrin (Julien et al., 2010), suggesting that metabolic impairment can trigger synaptic deficits. Our investigation sought to determine whether insulin deficiency could exacerbate synaptic

impairment in 3xTg-AD mice. In young 3xTg-AD mice, we observed that STZ-induced insulin deficiency led to a reduction in pre-synaptic synaptophysin and debrin levels. Hence, STZ-induced insulin deficiency precipitates synaptic deficits in young 3xTg-AD mice, concomitantly with the exacerbation of both A $\beta$  and tau accumulation. However, STZ treatment did not exacerbate the age-dependent synaptic deficits in 23-month-old 3xTg-AD mice. Again, the potentiation of existing pronounced synaptic deficits in older 3xTg-AD mice may present considerable challenges. Finally, we assessed central insulin signaling pathways to determine whether the observed tau hyperphosphorylation might be a consequence of central insulin dysfunction following peripheral insulin impairment. The reduction in PI3K, a pivotal component of insulin signaling, observed in 23-month-old 3xTg-AD mice is consistent with previous studies (Li et al., 2007; Jolivald et al., 2008, 2010). Given that PI3K can inhibit GSK-3 $\beta$  and possesses neuroprotective properties against AD pathophysiology (Razani et al., 2021), the age-dependent reduction in PI3K expression in 3xTg-AD mice could exacerbate tau pathology. Interestingly, we observed contrasting results in 7-month-old 3xTg-AD mice, characterized by an increase in IR phosphorylation and PI3K expression following STZ administration. These observations might be a consequence of either central insulin production to counteract severe hyperglycemia, or an acute compensatory mechanism to face insulin-resistance within the brain – that might not be long-lasting – as previously reported in this model (Sun et al., 2018). These findings warrant further investigations, especially for analyzing the long-term consequences of inducing insulin deficiency in young 3xTg-AD on AD pathophysiology.

In conclusion, our work unveils age-dependent sensitivity to STZ administration in 3xTg-AD mice. Intraperitoneal injection of STZ induced pronounced insulin deficiency-related symptoms in young mice alongside increased A $\beta$  and tau accumulation, without changes in tau phosphorylation. In contrast, aged 3xTg-AD mice appeared more resilient to insulin deficiency while exhibiting exacerbated tau pathology, involving dysregulation in both CDK5 and PP2A activities. These changes are likely attributable to the dysfunction of the BBB in aged 3xTg-AD mice, enabling the direct neurotoxic effects of STZ within the brain. It is not entirely unexpected that most of the pathological alterations observed in 23-month-old 3xTg-AD mice can be ascribed to a direct effect of STZ, given that intracerebroventricular infusion of STZ is a widely-recognized method for inducing AD pathology in rodents (Ravelli et al., 2017; Silva et al., 2023). Our results substantiate an association between insulin dysfunction, tau pathology, and AD, suggesting potential therapeutic targets for conditions involving both AD and diabetes.

## ACKNOWLEDGMENTS

We would like to thank the late Dr. Peter Davies (Albert Einstein College of Medicine, Bronx, NY, USA) for the gift of the MC6, PHF1 and TG3 antibodies and Dr. Peter Seubert (Elan Pharmaceuticals) for the gift of the 12E8 antibody.

## FUNDING

This work was supported by grants to E.P. from the CIHR (MOP-106423, PCN-102993), the NSERC (354722), the FRQS (16205, 20048). G.C. and C.J. were supported by Postdoctoral Awards from the Alzheimer Society of Canada and the Alzheimer Society of Saskatchewan. M.G. and N.B.E.K. were supported by Doctoral Awards from the Alzheimer Society of Canada.

## DECLARATION OF GENERATIVE AI AND AI-ASSISTED TECHNOLOGIES IN THE WRITING PROCESS

During the preparation of this work the authors used ChatGPT v4.0 in order to improve readability and language. After using this tool/service, the authors reviewed and edited the content as needed and take(s) full responsibility for the content of the publication.

## CONFLICTS OF INTERESTS

No potential conflicts of interest relevant to this article were reported

## AUTHOR CONTRIBUTIONS

C.J. and E.P. conceived the experimental design and wrote the manuscript. C.J. also performed experiments and analyzed data. G.C. performed experiments, helped with data analysis and figures presentation, and wrote the manuscript. M.G, C.Z., N.B.E.K. and M.L.B. helped with the experiments and corrected the manuscript. C.T. performed the insulin ELISA. F.M. helped with animal experiments. F.C. provided expertise for A $\beta$  analysis. S.S.H. provided assistance and corrected the manuscript. All authors reviewed and approved the final manuscript. C.J. and E.P. are the guarantors of this work and, as such, had full access to all the data in the study and takes responsibility for the integrity of the data and the accuracy of the data analysis.

**Table 1: Antibodies used in Western blot experiments**

Protein	Species	Dilution	Catalog	Supplier
<b>Total tau</b>				
TauC (amino acids 243-441)	Rabbit	1/10000	A0024	Dako Cytomation
CP27 (human tau)	Mouse	1/1000	-	Peter Davies
<b>Phosphorylated tau</b>				
AT8 (pSer202/pThr205)	Mouse	1/1000	MN1020	ThermoFisher
AT180 (pThr231/pSer235)	Mouse	1/1000	MN1040	ThermoFisher
MC6 (pSer235)	Mouse	1/1000	-	Peter Davies
PHF1 (pSer396/pSer404)	Mouse	1/1000	-	Peter Davies
AT270 (pThr181)	Mouse	1/1000	MN1050	ThermoFisher
Tau-1 (non-pSer195/Ser198/Ser199/Ser202)	Mouse	1/1000	MAB3420	Millipore
TG3	Mouse	1/1000	-	Peter Davies
12E8	Mouse	1/1000	-	Peter Seubert
CP13	Mouse	1/1000	-	Peter Davies
pS404	Rabbit	1/1000	44-758G	ThermoFisher
pS422	Rabbit	1/1000	44-764G	ThermoFisher
<b>Kinases</b>				
GSK-3 $\beta$ (Glycogen Synthase Kinase 3 $\beta$ )	Mouse	1/1000	610202	BD Biosciences
pGSK-3 $\beta$ (Ser9)	Rabbit	1/1000	9336S	Cell Signaling
AKT (Protein B Kinase)	Rabbit	1/1000	BS-6951R-FITC	ThermoFisher
pAKT (Ser473)	Mouse	1/1000	12-9715-42	ThermoFisher
ERK/MAPK (Extracellular signal-Regulated Kinase)	Rabbit	1/1000	44-654G	ThermoFisher
pERK (Thr202/pTyr204)	Mouse	1/1000	14-91-09-82	ThermoFisher
JNK/SAPK (c-Jun N-terminal Kinase)	Rabbit	1/1000	9252S	Cell Signaling
pJNK (Thr183/Tyr185)	Rabbit	1/1000	9251S	Cell Signaling
CDK5 (Cyclin-Dependent Kinase 5)	Rabbit	1/1000	2506S	Cell Signaling
p35 / p25	Rabbit	1/1000	2680S	Cell Signaling
CAMKII (Ca <sup>2+</sup> /calmodulin-dependent protein Kinase II)	Mouse	1/1000	Sc-5306	Santa-Cruz
pCAMKII (Thr286)	Rabbit	1/1000	Sc-12886	Santa-Cruz
<b>Phosphatases</b>				
PP1 (Protein Phosphatase 1)	Mouse	1/1000	Sc-7482	Santa-Cruz
PP2B / calcineurin A ( $\alpha$ isoform)	Rabbit	1/1000	PA5-29255	ThermoFisher
PP2A ( $\alpha$ and $\beta$ )	Rabbit	1/1000	PA517980	ThermoFisher
PP2A C ( $\alpha$ and $\beta$ )	Rabbit	1/1000	13482-1-AP	ThermoFisher
Demethylated PP2A C	Mouse	1/1000	Sc-13601	Santa-Cruz
PP2A-B $\alpha$	Mouse	1/1000	MA5-18064	ThermoFisher
PP2A-B $\beta$	Rabbit	1/1000	BS-11749R	ThermoFisher
PP5	Rabbit	1/1000	PA112682	ThermoFisher
<b>Amyloid markers</b>				
APP / C99	Rabbit	1/1000	PA1-84165	ThermoFisher
BACE1 (D10E5)	Rabbit	1/1000	5606S	Cell Signaling
<b>Synaptic markers</b>				
Drebrin (M2F6)	Mouse	1/5000	ALEXADI-NBA-110-E	VWR
PSD95 (K28/43)	Mouse	1/2000	MABN68	Millipore
Synaptophysin (SVP38)	Mouse	1/10000	SAB4200544	Millipore

SNAP-25 (SMI81)	Mouse	1/1000	SMI81-R	Covance
<b>Insulin pathway</b>				
IR (Insulin Receptor $\beta$ )	Mouse	1/1000	sc-57342	Santa-Cruz
pIR (Tyr972)	Rabbit	1/1000	l1783	Millipore
PI3K	Rabbit	1/1000	4292S	Cell Signaling
pPI3K (Tyr458/Tyr199)	Rabbit	1/1000	4228S	Cell Signaling
IDE	Rabbit	1/1000	ab32216	Abcam
<b>Blood-brain barrier marker</b>				
ZO1	Rabbit	1/1000	61-7300	ThermoFisher
VE-Cadherin	Rabbit	1/1000	ab33168	Abcam
Occludin	Rabbit	1/250	71-1500	Millipore/Sigma
<b>Loading control</b>				
$\beta$ -actin	Mouse	1/10000	A2628	Sigma-Aldrich
<b>Secondary antibodies</b>				
HRP conjugate goat anti-mouse IgG (HC+LC)	1/5000	1/5000	115-035-003	Jackson laboratories
HRP conjugate goat anti-mouse IgG (LC specific)	1/5000	1/5000	AP200P	Millipore
HRP conjugate goat anti-rabbit IgG (HC+LC)	1/5000	1/5000	111-035-144	Jackson laboratories

**Table 2: Summary of animal studies showing AD-related pathology following streptozotocin injection**

Animal Model	Age (months)	STZ-induced (i.p.)	Time of euthanasia post-induction	Insulin signaling	Tau phosphorylation sites	Tau enzymes	Amyloid burden	Anesthesia prior to sacrifice	Reference
C57/BL6 (♂)	1.5	150 mg/kg	3 days	(-) insulinemia	(+) AT8, AT180, AT270, PHF1, 12E8, S199, T212 (-) Tau1	(+) pJNK, p(S9)GSK3β (-) PP2A	N.D.	N.R.	(Clodfelder-Miller et al., 2006)
C57/BL6 (♂)	3-6	200 mg/kg	10-20-30-40 days	(+) glycemia	(+) AT8, AT180, PHF1, S199, S422, S262, S356, S400 (-) Tau1	(+) pCamKII, pJNK, p(S9)GSK3β (-) PP2A	(=) APP, APP-CTF, Aβ1-40/1-42	No	(Planel et al., 2007b)
C57/BL6 (♂)	4	150 mg/kg	4 months	(+) glycemia (=) insulinemia	(+) T231, S199, S202, S396	N.D.	N.D.	Yes	(Kim et al., 2009)
C57/BL6 (♂)	1.5-2	200 mg/kg	24 days	(+) glycemia	(+) S356, Tau5	N.D.	(+) Aβ1-42	Yes	(Ding et al., 2021)
Swiss-Webster (♂)	N.R.	90 mg/kg/day for 2 days	9 weeks	(-) pIR, PDK1, IDE	(+) T231, PHF1	(-) p(S9)GSK3β, pAKT	(+) Aβ (=) APP, APP-CTF	Yes	(Jolivalt et al., 2008)
Sprague-Dawley (♂)	4	55 mg/kg	30 days	(-) insulinemia	(+) PHF1 (-) Tau1	(-) p(S9)GSK3β, pAKT, PP2A	N.D.	N.R.	(Qu et al., 2011)
h-APP (♂)	4	90 mg/kg/day for 2 days	9 weeks	(+) glycemia (-) pIR, IDE	(+) T231, AT8, PHF1	(-) p(S9)GSK3β (+) p(Y216)GSK3β	(+) APP, Aβ, Aβ plaques	Yes	(Jolivalt et al., 2010)
pR5 (♂)	4	200 mg/kg	2 months	(+) glycemia (-) insulinemia	(+) AT100, AT8, AT270, 12E8, PHF1, S422	N.D.	N.D.	N.R.	(Ke et al., 2009)
3xTg-AD (♂)	6	50 mg/kg/day for 5 days	3 months	(+) pIR	(+) AT8, AT180	(-) pAkt, p(S9)GSK3β (=) pAkt	(+) Aβ1-42	N.R.	(Imamura et al., 2020)
3xTg-AD	3	60 mg/kg/day for 5 days	8 weeks	(+) glycemia	(+) S396, T231 (=) Tau5	(-) pAMPK	N.D.	Yes	(Wang et al., 2020)
APP/PS1 (♂)	3	90 mg/kg/day for 2 days	4.5 months	(+) glycemia (-) insulinemia, pIR	N.D.	(+) pJNK (-) p(S9)GSK3β, pGSK3α	(+) sAPPβ, APP-CTF, BACE1 (+) Aβ plaques, Aβ1-42	Yes	(Wang et al., 2010)
Tg2576 (♀)	3	50 mg/kg/day for 5 days	4 months	(+) glycemia (-) insulinemia (-) pIR, IDE	(+) T231, AT8	(+) pERK, p(S9)GSK3β	(+) Aβ plaques, Aβ1-40/1-42	Yes	(Zhou et al., 2022)
5xFAD-AD	1.5	90 mg/kg/day for 2 days	2.5 months	(-) insulinemia	N.D.	N.D.	(+) APP, C99, BACE1 (+) Aβ plaques, Aβ1-40/1-42 (-) sAPPα	Yes	(Devi et al., 2012)
hTau (♂♀)	14-15	75 mg/kg for 2 days	1 month	N.D.	(+) AT8 (=) AT180, AT270, PHF1	(+) CaMKII (=) CDK5, ERK, MAPK, (-) p(S9)GSK3β	N.D.	N.R.	(Trujillo-Estrada et al., 2019)

---

7-9	50 mg/kg/day for 5 days	4 weeks	(+) glycemia (-) insulinemia	(+) AT8, AT180, T205, PHF1, CP13 (-) Tau1	(=) PP1, PP2B, PP5, PTEN, AKT, PI3K, (-) pCaMKII, JNK, p38, ERK cdk5, PP2A (+) p(S9)GSK3 $\beta$	N.D.	No	(Gratuze et al., 2017)
-----	-------------------------	---------	---------------------------------	--	---	------	----	------------------------

---

Journal Pre-proof

## REFERENCES

- Alonso, A. D. C., Grundke-Iqbal, I., and Iqbal, K. (1996). Alzheimer's disease hyperphosphorylated tau sequesters normal tau into tangles of filaments and disassembles microtubules. *Nat Med* 2, 783–787. doi: 10.1038/nm0796-783
- Alonso, A. d. C., Zaidi, T., Novak, M., Grundke-Iqbal, I., and Iqbal, K. (2001). Hyperphosphorylation induces self-assembly of into tangles of paired helical filaments/straight filaments. *Proceedings of the National Academy of Sciences* 98, 6923–6928. doi: 10.1073/pnas.121119298
- Augustinack, J. C., Schneider, A., Mandelkow, E.-M., and Hyman, B. T. (2002). Specific tau phosphorylation sites correlate with severity of neuronal cytopathology in Alzheimer's disease. *Acta Neuropathol* 103, 26–35. doi: 10.1007/s004010100423
- Baharians, Z., and Schönthal, A. H. (1998). Autoregulation of Protein Phosphatase Type 2A Expression. *Journal of Biological Chemistry* 273, 19019–19024. doi: 10.1074/jbc.273.30.19019
- Barbagallo, M., and Dominguez, L. J. (2014). Type 2 diabetes mellitus and Alzheimer's disease. *WJD* 5, 889. doi: 10.4239/wjd.v5.i6.889
- Billings, L. M., Oddo, S., Green, K. N., McGaugh, J. L., and LaFerla, F. M. (2005). Intraneuronal A $\beta$  Causes the Onset of Early Alzheimer's Disease-Related Cognitive Deficits in Transgenic Mice. *Neuron* 45, 675–688. doi: 10.1016/j.neuron.2005.01.040
- Bourasset, F., Ouellet, M., Tremblay, C., Julien, C., Do, T. M., Oddo, S., et al. (2009). Reduction of the cerebrovascular volume in a transgenic mouse model of Alzheimer's disease. *Neuropharmacology* 56, 808–813. doi: 10.1016/j.neuropharm.2009.01.006
- Canet, G., Rocaboy, E., Diego-Diàz, S., Whittington, R. A., Julien, C., and Planel, E. (2024). “Methods for Biochemical Isolation of Insoluble Tau in Rodent Models of Tauopathies,” in *Tau Protein*, ed. C. Smet-Nocca (New York, NY: Springer US), 323–341. doi: 10.1007/978-1-0716-3629-9\_17
- Canet, G., Rocaboy, E., Laliberté, F., Boscher, E., Guisle, I., Diego-Diaz, S., et al. (2023). Temperature-induced Artifacts in Tau Phosphorylation: Implications for Reliable Alzheimer's Disease Research. *Exp Neurobiol* 32, 423–440. doi: 10.5607/en23025
- Carvalho, C., Santos, M. S., Oliveira, C. R., and Moreira, P. I. (2015). Alzheimer's disease and type 2 diabetes-related alterations in brain mitochondria, autophagy and synaptic markers. *Biochimica et Biophysica Acta (BBA) - Molecular Basis of Disease* 1852, 1665–1675. doi: 10.1016/j.bbadis.2015.05.001
- Chen, Y., Liang, Z., Tian, Z., Blanchard, J., Dai, C., Chalbot, S., et al. (2014). Intracerebroventricular Streptozotocin Exacerbates Alzheimer-Like Changes of 3xTg-AD Mice. *Mol Neurobiol* 49, 547–562. doi: 10.1007/s12035-013-8539-y
- Clodfelder-Miller, B. J., Zmijewska, A. A., Johnson, G. V. W., and Jope, R. S. (2006). Tau Is Hyperphosphorylated at Multiple Sites in Mouse Brain In Vivo After Streptozotocin-Induced Insulin Deficiency. *Diabetes* 55, 3320–3325. doi: 10.2337/db06-0485
- Craft, S., and Stennis Watson, G. (2004). Insulin and neurodegenerative disease: shared and specific mechanisms. *The Lancet Neurology* 3, 169–178. doi: 10.1016/S1474-4422(04)00681-7

- Devi, L., Alldred, M. J., Ginsberg, S. D., and Ohno, M. (2012). Mechanisms Underlying Insulin Deficiency-Induced Acceleration of  $\beta$ -Amyloidosis in a Mouse Model of Alzheimer's Disease. *PLoS ONE* 7, e32792. doi: 10.1371/journal.pone.0032792
- Di Meco, A., Joshi, Y. B., and Praticò, D. (2014). Sleep deprivation impairs memory, tau metabolism, and synaptic integrity of a mouse model of Alzheimer's disease with plaques and tangles. *Neurobiology of Aging* 35, 1813–1820. doi: 10.1016/j.neurobiolaging.2014.02.011
- Ding, Y., Liu, H., Cen, M., Tao, Y., Lai, C., and Tang, Z. (2021). Rapamycin Ameliorates Cognitive Impairments and Alzheimer's Disease-Like Pathology with Restoring Mitochondrial Abnormality in the Hippocampus of Streptozotocin-Induced Diabetic Mice. *Neurochem Res* 46, 265–275. doi: 10.1007/s11064-020-03160-6
- Do, T. M., Alata, W., Dodacki, A., Traversy, M.-T., Chacun, H., Pradier, L., et al. (2014). Altered cerebral vascular volumes and solute transport at the blood–brain barriers of two transgenic mouse models of Alzheimer's disease. *Neuropharmacology* 81, 311–317. doi: 10.1016/j.neuropharm.2014.02.010
- Erdő, F., Denes, L., and De Lange, E. (2017). Age-associated physiological and pathological changes at the blood–brain barrier: A review. *J Cereb Blood Flow Metab* 37, 4–24. doi: 10.1177/0271678X16679420
- Fereydouni-Forouzandeh, P., Canet, G., Diego-Diàz, S., Rocaboy, E., Petry, S., Whittington, R. A., et al. (2024). “Western Blot of Tau Protein from Mouse Brains Extracts: How to Avoid Signal Artifacts,” in *Tau Protein*, ed. C. Smet-Nocca (New York, NY: Springer US), 309–321. doi: 10.1007/978-1-0716-3629-9\_16
- Frölich, L., Blum-Degen, D., Riederer, P., and Hoyer, S. (1999). A Disturbance in the Neuronal Insulin Receptor Signal Transduction in Sporadic Alzheimer's Disease. *Annals of the New York Academy of Sciences* 893, 290–293. doi: 10.1111/j.1749-6632.1999.tb07839.x
- Ganda, O. P., Rossini, A. A., and Like, A. A. (1976). Studies on Streptozotocin Diabetes. *Diabetes* 25, 595–603. doi: 10.2337/diab.25.7.595
- Gasparini, L. (2002). Does insulin dysfunction play a role in Alzheimer's disease? *Trends in Pharmacological Sciences* 23, 288–293. doi: 10.1016/S0165-6147(02)02037-0
- Goedert, M., Jakes, R., Crowther, R. A., Cohen, P., Vanmechelen, E., Vandermeeren, M., et al. (1994). Epitope mapping of monoclonal antibodies to the paired helical filaments of Alzheimer's disease: identification of phosphorylation sites in tau protein. *Biochem J* 301 ( Pt 3), 871–877. doi: 10.1042/bj3010871
- Goedert, M., Jakes, R., Qi, Z., Wang, J. H., and Cohen, P. (1995). Protein Phosphatase 2A Is the Major Enzyme in Brain that Dephosphorylates  $\tau$  Protein Phosphorylated by Proline-Directed Protein Kinases or Cyclic AMP-Dependent Protein Kinase. *Journal of Neurochemistry* 65, 2804–2807. doi: 10.1046/j.1471-4159.1995.65062804.x
- Gong, C., Singh, T. J., Grundke-Iqbal, I., and Iqbal, K. (1993). Phosphoprotein Phosphatase Activities in Alzheimer Disease Brain. *Journal of Neurochemistry* 61, 921–927. doi: 10.1111/j.1471-4159.1993.tb03603.x
- Gratuze, M., Joly-Amado, A., Buee, L., Vieau, D., and Blum, D. (2019). Tau, Diabetes and Insulin. *Adv Exp Med Biol* 1184, 259–287. doi: 10.1007/978-981-32-9358-8\_21

- Gratuze, M., Julien, J., Petry, F. R., Morin, F., and Planel, E. (2017). Insulin deprivation induces PP2A inhibition and tau hyperphosphorylation in hTau mice, a model of Alzheimer's disease-like tau pathology. *Sci Rep* 7, 46359. doi: 10.1038/srep46359
- Greenberg, S. G., and Davies, P. (1990). A preparation of Alzheimer paired helical filaments that displays distinct tau proteins by polyacrylamide gel electrophoresis. *Proc. Natl. Acad. Sci. U.S.A.* 87, 5827–5831. doi: 10.1073/pnas.87.15.5827
- Grieb, P. (2016). Intracerebroventricular Streptozotocin Injections as a Model of Alzheimer's Disease: in Search of a Relevant Mechanism. *Mol Neurobiol* 53, 1741–1752. doi: 10.1007/s12035-015-9132-3
- Griffith, C. M., Macklin, L. N., Cai, Y., Sharp, A. A., Yan, X.-X., Reagan, L. P., et al. (2019). Impaired Glucose Tolerance and Reduced Plasma Insulin Precede Decreased AKT Phosphorylation and GLUT3 Translocation in the Hippocampus of Old 3xTg-AD Mice. *JAD* 68, 809–837. doi: 10.3233/JAD-180707
- Grünblatt, E., Salkovic-Petrisic, M., Osmanovic, J., Riederer, P., and Hoyer, S. (2007). Brain insulin system dysfunction in streptozotocin intracerebroventricularly treated rats generates hyperphosphorylated tau protein. *Journal of Neurochemistry* 101, 757–770. doi: 10.1111/j.1471-4159.2006.04368.x
- Haj-Yahya, M., Gopinath, P., Rajasekhar, K., Mirbaha, H., Diamond, M. I., and Lashuel, H. A. (2020). Site-Specific Hyperphosphorylation Inhibits, Rather than Promotes, Tau Fibrillization, Seeding Capacity, and Its Microtubule Binding. *Angew Chem Int Ed* 59, 4059–4067. doi: 10.1002/anie.201913001
- Hayashi-Park, E., Ozment, B. N., Griffith, C. M., Zhang, H., Patrylo, P. R., and Rose, G. M. (2017). Experimentally induced diabetes worsens neuropathology, but not learning and memory, in middle aged 3xTg mice. *Behavioural Brain Research* 322, 280–287. doi: 10.1016/j.bbr.2016.05.020
- Hoffman, A., Taleski, G., and Sontag, E. (2017). The protein serine/threonine phosphatases PP2A, PP1 and calcineurin: A triple threat in the regulation of the neuronal cytoskeleton. *Molecular and Cellular Neuroscience* 84, 119–131. doi: 10.1016/j.mcn.2017.01.005
- Hsueh, W., Abel, E. D., Breslow, J. L., Maeda, N., Davis, R. C., Fisher, E. A., et al. (2007). Recipes for Creating Animal Models of Diabetic Cardiovascular Disease. *Circulation Research* 100, 1415–1427. doi: 10.1161/01.RES.0000266449.37396.1f
- Imamura, T., Yanagihara, Y. T., Ohyagi, Y., Nakamura, N., Iinuma, K. M., Yamasaki, R., et al. (2020). Insulin deficiency promotes formation of toxic amyloid- $\beta$ 42 conformer co-aggregating with hyper-phosphorylated tau oligomer in an Alzheimer's disease model. *Neurobiology of Disease* 137, 104739. doi: 10.1016/j.nbd.2020.104739
- Islas-Hernandez, A., and Garcia-Delatorre, P. (2020). Integrity of the blood-brain barrier and changes in the microvasculature during the progression of Alzheimer's disease in the 3XTG-AD model: Molecular and cell biology/vascular factors. *Alzheimer's & Dementia* 16, e044346. doi: 10.1002/alz.044346
- Jicha, G. A., Bowser, R., Kazam, I. G., and Davies, P. (1997). Alz-50 and MC-1, a new monoclonal antibody raised to paired helical filaments, recognize conformational epitopes on recombinant tau. *J Neurosci Res* 48, 128–132. doi: 10.1002/(sici)1097-4547(19970415)48:2<128::aid-jnr5>3.0.co;2-e

- Jolival, C. G., Hurford, R., Lee, C. A., Dumaop, W., Rockenstein, E., and Masliah, E. (2010). Type 1 diabetes exaggerates features of Alzheimer's disease in APP transgenic mice. *Experimental Neurology* 223, 422–431. doi: 10.1016/j.expneurol.2009.11.005
- Jolival, C. G., Lee, C. A., Beiswenger, K. K., Smith, J. L., Orlov, M., Torrance, M. A., et al. (2008). Defective insulin signaling pathway and increased glycogen synthase kinase-3 activity in the brain of diabetic mice: Parallels with Alzheimer's disease and correction by insulin. *J of Neuroscience Research* 86, 3265–3274. doi: 10.1002/jnr.21787
- Julien, C., Tremblay, C., Phivilay, A., Berthiaume, L., Émond, V., Julien, P., et al. (2010). High-fat diet aggravates amyloid-beta and tau pathologies in the 3xTg-AD mouse model. *Neurobiology of Aging* 31, 1516–1531. doi: 10.1016/j.neurobiolaging.2008.08.022
- Ke, Y. D., Delerue, F., Gladbach, A., Götz, J., and Ittner, L. M. (2009). Experimental Diabetes Mellitus Exacerbates Tau Pathology in a Transgenic Mouse Model of Alzheimer's Disease. *PLoS ONE* 4, e7917. doi: 10.1371/journal.pone.0007917
- Kim, B., Backus, C., Oh, S., Hayes, J. M., and Feldman, E. L. (2009). Increased Tau Phosphorylation and Cleavage in Mouse Models of Type 1 and Type 2 Diabetes. *Endocrinology* 150, 5294–5301. doi: 10.1210/en.2009-0695
- Kimura, T., Ishiguro, K., and Hisanaga, S. (2014). Physiological and pathological phosphorylation of tau by Cdk5. *Front. Mol. Neurosci.* 7. doi: 10.3389/fnmol.2014.00065
- Koepsell, H. (2020). Glucose transporters in brain in health and disease. *Pflugers Arch - Eur J Physiol* 472, 1299–1343. doi: 10.1007/s00424-020-02441-x
- Korczyński, A. D., and Grinberg, L. T. (2024). Is Alzheimer disease a disease? *Nat Rev Neurol* 20, 245–251. doi: 10.1038/s41582-024-00940-4
- Leclerc, M., Bourassa, P., Tremblay, C., Caron, V., Sugère, C., Emond, V., et al. (2023). Cerebrovascular insulin receptors are defective in Alzheimer's disease. *Brain* 146, 75–90. doi: 10.1093/brain/awac309
- Leclerc, M., Dudonné, S., and Calon, F. (2021). Can Natural Products Exert Neuroprotection without Crossing the Blood–Brain Barrier? *IJMS* 22, 3356. doi: 10.3390/ijms22073356
- Li, Z., Zhang, W., and Sima, A. A. F. (2007). Alzheimer-Like Changes in Rat Models of Spontaneous Diabetes. *Diabetes* 56, 1817–1824. doi: 10.2337/db07-0171
- Litersky, J. M., Johnson, G. V. W., Jakes, R., Goedert, M., Lee, M., and Seubert, P. (1996). Tau protein is phosphorylated by cyclic AMP-dependent protein kinase and calcium/calmodulin-dependent protein kinase II within its microtubule-binding domains at Ser-262 and Ser-356. *Biochemical Journal* 316, 655–660. doi: 10.1042/bj3160655
- Liu, Y., Liu, H., Yang, J., Liu, X., Lu, S., Wen, T., et al. (2008). Increased amyloid  $\beta$ -peptide (1–40) level in brain of streptozotocin-induced diabetic rats. *Neuroscience* 153, 796–802. doi: 10.1016/j.neuroscience.2008.03.019
- Long, J. M., and Holtzman, D. M. (2019). Alzheimer Disease: An Update on Pathobiology and Treatment Strategies. *Cell* 179, 312–339. doi: 10.1016/j.cell.2019.09.001
- Macauley, S. L., Stanley, M., Caesar, E. E., Yamada, S. A., Raichle, M. E., Perez, R., et al. (2015). Hyperglycemia modulates extracellular amyloid- $\beta$  concentrations and neuronal activity in vivo. *J. Clin. Invest.* 125, 2463–2467. doi: 10.1172/JCI79742

- Martin, L., Latypova, X., Wilson, C. M., Magnaudeix, A., Perrin, M.-L., and Terro, F. (2013a). Tau protein phosphatases in Alzheimer's disease: The leading role of PP2A. *Ageing Research Reviews* 12, 39–49. doi: 10.1016/j.arr.2012.06.008
- Martin, L., Latypova, X., Wilson, C. M., Magnaudeix, A., Perrin, M.-L., Yardin, C., et al. (2013b). Tau protein kinases: Involvement in Alzheimer's disease. *Ageing Research Reviews* 12, 289–309. doi: 10.1016/j.arr.2012.06.003
- Mehta, D. C., Short, J. L., and Nicolazzo, J. A. (2013). Altered Brain Uptake of Therapeutics in a Triple Transgenic Mouse Model of Alzheimer's Disease. *Pharm Res* 30, 2868–2879. doi: 10.1007/s11095-013-1116-2
- Mercken, M., Vandermeeren, M., Lübke, U., Six, J., Boons, J., Van De Voorde, A., et al. (1992). Monoclonal antibodies with selective specificity for Alzheimer Tau are directed against phosphatase-sensitive epitopes. *Acta Neuropathol* 84, 265–272. doi: 10.1007/BF00227819
- Noble, W., Olm, V., Takata, K., Casey, E., Mary, O., Meyerson, J., et al. (2003). Cdk5 Is a Key Factor in Tau Aggregation and Tangle Formation In Vivo. *Neuron* 38, 555–565. doi: 10.1016/S0896-6273(03)00259-9
- Oddo, S., Caccamo, A., Shepherd, J. D., Murphy, M. P., Golde, T. E., Kaye, R., et al. (2003). Triple-transgenic model of Alzheimer's disease with plaques and tangles: intracellular Abeta and synaptic dysfunction. *Neuron* 39, 409–421.
- Ott, A., Stolk, R. P., Van Harskamp, F., Pols, H. A. P., Hofman, A., and Breteler, M. M. B. (1999). Diabetes mellitus and the risk of dementia: The Rotterdam Study. *Neurology* 53, 1937–1937. doi: 10.1212/WNL.53.9.1937
- Otvos, L., Feiner, L., Lang, E., Szendrei, G. I., Goedert, M., and Lee, V. M. (1994). Monoclonal antibody PHF-1 recognizes tau protein phosphorylated at serine residues 396 and 404. *J of Neuroscience Research* 39, 669–673. doi: 10.1002/jnr.490390607
- Papon, M.-A., El Khoury, N. B., Marcouiller, F., Julien, C., Morin, F., Bretteville, A., et al. (2013). Deregulation of Protein Phosphatase 2A and Hyperphosphorylation of  $\tau$  Protein Following Onset of Diabetes in NOD Mice. *Diabetes* 62, 609–617. doi: 10.2337/db12-0187
- Planel, E., Bretteville, A., Liu, L., Virag, L., Du, A. L., Yu, W. H., et al. (2009). Acceleration and persistence of neurofibrillary pathology in a mouse model of tauopathy following anesthesia. *FASEB j.* 23, 2595–2604. doi: 10.1096/fj.08-122424
- Planel, E., Richter, K. E. G., Nolan, C. E., Finley, J. E., Liu, L., Wen, Y., et al. (2007a). Anesthesia Leads to Tau Hyperphosphorylation through Inhibition of Phosphatase Activity by Hypothermia. *Journal of Neuroscience* 27, 3090–3097. doi: 10.1523/JNEUROSCI.4854-06.2007
- Planel, E., Sun, X., and Takashima, A. (2002). Role of GSK-3 $\beta$  in Alzheimer's disease pathology. *Drug Dev. Res.* 56, 491–510. doi: 10.1002/ddr.10100
- Planel, E., Tatebayashi, Y., Miyasaka, T., Liu, L., Wang, L., Herman, M., et al. (2007b). Insulin Dysfunction Induces In Vivo Tau Hyperphosphorylation through Distinct Mechanisms. *Journal of Neuroscience* 27, 13635–13648. doi: 10.1523/JNEUROSCI.3949-07.2007
- Planel, E., Yasutake, K., Fujita, S. C., and Ishiguro, K. (2001). Inhibition of Protein Phosphatase 2A Overrides Tau Protein Kinase I/Glycogen Synthase Kinase 3 $\beta$  and Cyclin-dependent Kinase

- 5 Inhibition and Results in Tau Hyperphosphorylation in the Hippocampus of Starved Mouse. *Journal of Biological Chemistry* 276, 34298–34306. doi: 10.1074/jbc.M102780200
- Plaschke, K., Kopitz, J., Siegelin, M., Schliebs, R., Salkovic-Petrisic, M., Riederer, P., et al. (2010). Insulin-Resistant Brain State after Intracerebroventricular Streptozotocin Injection Exacerbates Alzheimer-like Changes in Tg2576 A $\beta$ PP-Overexpressing Mice. *JAD* 19, 691–704. doi: 10.3233/JAD-2010-1270
- Pollak, D., Cairns, N., and Lubec, G. (2003). “Cytoskeleton derangement in brain of patients with Down Syndrome, Alzheimer’s disease and Pick’s disease,” in *Advances in Down Syndrome Research*, ed. G. Lubec (Vienna: Springer Vienna), 149–158. doi: 10.1007/978-3-7091-6721-2\_13
- Pugazhenthii, S., Qin, L., and Reddy, P. H. (2017). Common neurodegenerative pathways in obesity, diabetes, and Alzheimer’s disease. *Biochimica et Biophysica Acta (BBA) - Molecular Basis of Disease* 1863, 1037–1045. doi: 10.1016/j.bbadis.2016.04.017
- Qu, Z., Jiao, Z., Sun, X., Zhao, Y., Ren, J., and Xu, G. (2011). Effects of streptozotocin-induced diabetes on tau phosphorylation in the rat brain. *Brain Research* 1383, 300–306. doi: 10.1016/j.brainres.2011.01.084
- Querfurth, H. W., and LaFerla, F. M. (2010). Alzheimer’s disease. *N. Engl. J. Med.* 362, 329–344. doi: 10.1056/NEJMra0909142
- Ramos-Lobo, A. M., Buonfiglio, D. C., and Cipolla-Neto, J. (2015). Streptozotocin-induced diabetes disrupts the body temperature daily rhythm in rats. *Diabetol Metab Syndr* 7, 39. doi: 10.1186/s13098-015-0035-2
- Ravelli, K. G., Rosário, B. D. A., Camarini, R., Hernandes, M. S., and Britto, L. R. (2017). Intracerebroventricular Streptozotocin as a Model of Alzheimer’s Disease: Neurochemical and Behavioral Characterization in Mice. *Neurotox Res* 31, 327–333. doi: 10.1007/s12640-016-9684-7
- Razani, E., Pourbagheri-Sigaroodi, A., Safaroghli-Azar, A., Zoghi, A., Shanaki-Bavarsad, M., and Bashash, D. (2021). The PI3K/Akt signaling axis in Alzheimer’s disease: a valuable target to stimulate or suppress? *Cell Stress and Chaperones* 26, 871–887. doi: 10.1007/s12192-021-01231-3
- Rhea, E. M., Leclerc, M., Yassine, H. N., Capuano, A. W., Tong, H., Petyuk, V. A., et al. (2023). State of the Science on Brain Insulin Resistance and Cognitive Decline Due to Alzheimer’s Disease. *Aging and disease*, 0. doi: 10.14336/AD.2023.0814
- Riley, W. J., McConnell, T. J., McLaughlin, J. V., and Taylor, G. (1981). The Diabetogenic Effects of Streptozotocin in Mice are Prolonged and Inversely Related to Age. *Diabetes* 30, 718–723. doi: 10.2337/diab.30.9.718
- Rönnemaa, E., Zethelius, B., Sundelöf, J., Sundström, J., Degerman-Gunnarsson, M., Berne, C., et al. (2008). Impaired insulin secretion increases the risk of Alzheimer disease. *Neurology* 71, 1065–1071. doi: 10.1212/01.wnl.0000310646.32212.3a
- Sato, S., Tatebayashi, Y., Akagi, T., Chui, D.-H., Murayama, M., Miyasaka, T., et al. (2002). Aberrant Tau Phosphorylation by Glycogen Synthase Kinase-3 $\beta$  and JNK3 Induces Oligomeric Tau Fibrils in COS-7 Cells. *Journal of Biological Chemistry* 277, 42060–42065. doi: 10.1074/jbc.M202241200

- Schnedl, W. J., Ferber, S., Johnson, J. H., and Newgard, C. B. (1994). STZ Transport and Cytotoxicity: Specific Enhancement in GLUT2-Expressing Cells. *Diabetes* 43, 1326–1333. doi: 10.2337/diab.43.11.1326
- Selkoe, D. J. (2001). Alzheimer's disease: genes, proteins, and therapy. *Physiol. Rev.* 81, 741–766.
- Seubert, P., Mawal-Dewan, M., Barbour, R., Jakes, R., Goedert, M., Johnson, G. V. W., et al. (1995). Detection of Phosphorylated Ser262 in Fetal Tau, Adult Tau, and Paired Helical Filament Tau. *Journal of Biological Chemistry* 270, 18917–18922. doi: 10.1074/jbc.270.32.18917
- Silva, S. S. L., Tureck, L. V., Souza, L. C., Mello-Hortega, J. V., Piumbini, A. L., Teixeira, M. D., et al. (2023). Animal model of Alzheimer's disease induced by streptozotocin: New insights about cholinergic pathway. *Brain Research* 1799, 148175. doi: 10.1016/j.brainres.2022.148175
- Šimić, G., Babić Leko, M., Wray, S., Harrington, C., Delalle, I., Jovanov-Milošević, N., et al. (2016). Tau Protein Hyperphosphorylation and Aggregation in Alzheimer's Disease and Other Tauopathies, and Possible Neuroprotective Strategies. *Biomolecules* 6, 6. doi: 10.3390/biom6010006
- Sims-Robinson, C., Kim, B., Rosko, A., and Feldman, E. L. (2010). How does diabetes accelerate Alzheimer disease pathology? *Nat Rev Neurol* 6, 551–559. doi: 10.1038/nrneurol.2010.130
- Sun, P., Ortega, G., Tan, Y., Hua, Q., Riederer, P. F., Deckert, J., et al. (2018). Streptozotocin Impairs Proliferation and Differentiation of Adult Hippocampal Neural Stem Cells in Vitro—Correlation With Alterations in the Expression of Proteins Associated With the Insulin System. *Front Aging Neurosci* 10, 145. doi: 10.3389/fnagi.2018.00145
- Sweeney, M. D., Zhao, Z., Montagne, A., Nelson, A. R., and Zlokovic, B. V. (2019). Blood-Brain Barrier: From Physiology to Disease and Back. *Physiological Reviews* 99, 21–78. doi: 10.1152/physrev.00050.2017
- Szendrei, G. I., Lee, V. M. -Y., and Otvos, L. (1993). Recognition of the minimal epitope of monoclonal antibody Tau-1 depends upon the presence of a phosphate group but not its location. *J of Neuroscience Research* 34, 243–249. doi: 10.1002/jnr.490340212
- Tanzi, R. E., Moir, R. D., and Wagner, S. L. (2004). Clearance of Alzheimer's A $\beta$  Peptide. *Neuron* 43, 605–608. doi: 10.1016/j.neuron.2004.08.024
- Trayhurn, P. (1979). Thermoregulation in the diabetic-obese (db/db) mouse: The role of non-shivering thermogenesis in energy balance. *Pflugers Arch.* 380, 227–232. doi: 10.1007/BF00582901
- Trojanowski, J. Q., and Lee, V. M. (1994). Paired helical filament tau in Alzheimer's disease. The kinase connection. *Am J Pathol* 144, 449–453.
- Trujillo-Estrada, L., Gomez-Arboledas, A., Forner, S., Martini, A. C., Gutierrez, A., Baglietto-Vargas, D., et al. (2019). Astrocytes: From the Physiology to the Disease. *CAR* 16, 675–698. doi: 10.2174/1567205016666190830110152
- Vandal, M., White, P. J., Chevrier, G., Tremblay, C., St-Amour, I., Planel, E., et al. (2015). Age-dependent impairment of glucose tolerance in the 3xTg-AD mouse model of Alzheimer's disease. *FASEB j.* 29, 4273–4284. doi: 10.1096/fj.14-268482

- Wang, L., Li, N., Shi, F.-X., Xu, W.-Q., Cao, Y., Lei, Y., et al. (2020). Upregulation of AMPK Ameliorates Alzheimer's Disease-Like Tau Pathology and Memory Impairment. *Mol Neurobiol* 57, 3349–3361. doi: 10.1007/s12035-020-01955-w
- Wang, X., Zheng, W., Xie, J.-W., Wang, T., Wang, S.-L., Teng, W.-P., et al. (2010). Insulin deficiency exacerbates cerebral amyloidosis and behavioral deficits in an Alzheimer transgenic mouse model. *Mol Neurodegeneration* 5, 46. doi: 10.1186/1750-1326-5-46
- Weaver, C. (2000). Conformational change as one of the earliest alterations of tau in Alzheimer's disease. *Neurobiology of Aging* 21, 719–727. doi: 10.1016/S0197-4580(00)00157-3
- Wegmann, S., Biernat, J., and Mandelkow, E. (2021). A current view on Tau protein phosphorylation in Alzheimer's disease. *Current Opinion in Neurobiology* 69, 131–138. doi: 10.1016/j.conb.2021.03.003
- Whitmer, R. A., Gilsanz, P., Quesenberry, C. P., Karter, A. J., and Lacy, M. E. (2021). Association of Type 1 Diabetes and Hypoglycemic and Hyperglycemic Events and Risk of Dementia. *Neurology* 97. doi: 10.1212/WNL.00000000000012243
- Yoon, J. H., Hwang, J., Son, S. U., Choi, J., You, S.-W., Park, H., et al. (2023). How Can Insulin Resistance Cause Alzheimer's Disease? *Int J Mol Sci* 24, 3506. doi: 10.3390/ijms24043506
- Zhou, C., Jung, C.-G., Kim, M.-J., Watanabe, A., Abdelhamid, M., Taslima, F., et al. (2022). Insulin Deficiency Increases Sirt2 Level in Streptozotocin-Treated Alzheimer's Disease-Like Mouse Model: Increased Sirt2 Induces Tau Phosphorylation Through ERK Activation. *Mol Neurobiol* 59, 5408–5425. doi: 10.1007/s12035-022-02918-z

## LEGENDS

### **Figure 1. Streptozotocin (STZ) administration elicits insulin deficiency-related features only in 7-month-old 3xTg-AD mice.**

**a**, Experimental design: 7 or 23 months-old 3xTg-AD mice (males and females) were injected with Streptozotocin (50 mg/kg/day) for 5 consecutive days. Glycemia (mmol/L) was repeatedly monitored **b**, from 1 to 14 weeks post-STZ injections, and **c**, just before euthanasia in 7- and 23-months old 3xTg-mice. **d**, Maximum peak of glycemia (mM) recorded throughout the entire experimental period post-STZ injections. Note that while the glycemia of all the animals was recorded at the time of euthanasia, during the monitoring period it was not consistently recorded for each animal in the study, nor were measurements taken at uniform timepoints across different groups. **e**, Percentage of mice displaying glycosuria (presence of glucose in urine) following STZ injections. **f**, Insulinemia ( $\mu\text{g/L}$ ), **g**, Body weight (g) and, **h**, Rectal temperature ( $^{\circ}\text{C}$ ) were assessed just before euthanasia. Each individual in the data appears as a point on the graph. Data are presented as mean  $\pm$  SD. Two-way ANOVAs were performed followed by Tukey's post hoc test, or two separate t-tests between different groups of age. \* $p < 0.05$ , \*\* $p < 0.01$  and \*\*\* $p < 0.001$  vs. designated condition. CTL: non-treated control 3xTg-AD mice; STZ: 3xTg-AD mice subjected to STZ injections.

### **Figure 2. Streptozotocin (STZ) administration induced an age-dependent aggravation of cortical tau phosphorylation and accumulation in 3xTg-AD mice.**

Three months ( $14 \pm 1$  weeks) after STZ injections, tau phosphorylation was assessed by Western blot at the following epitopes: **a**, AT8 (pS202/pT205), **b**, PHF-1 (pS396/pS404), **c**, AT180 (pT231/pS235), **d**, Tau-1 (non-phosphorylated S195/S198/S199/S202), **e**, AT270 (pT181), **f**, CP13 (pS202), **g**, MC6 (pS235), **h**, pS199, **i**, pS404, **j**, pS422, **k**, TG3 (Thr231 conformational) and **l**, 12E8 (pS262) epitopes, and normalized to **m**, total tau levels using TauC antibody. The cortical levels of **n**, sarkosyl-insoluble tau was quantified by Western blot using TauC antibodies. Two representative lanes from each group of mice are displayed above the quantifications. Each individual in the data appears as a point on the graph. Data are presented as mean  $\pm$  SD and expressed as percentage of non-treated 7-months old 3xTg-AD mice (control group). Two-way ANOVAs were performed followed by Tukey's post hoc test. \* $p < 0.05$ , \*\* $p < 0.01$  and

\*\*\* $p < 0.001$  vs. designated condition. CTL: non-treated control 3xTg-AD mice; STZ: 3xTg-AD mice subjected to STZ injections.

**Figure 3. Streptozotocin (STZ) administration led to a moderate impairment in the cortical expression of tau-related kinases in 23-months old 3xTg-AD mice.**

Three months ( $14 \pm 1$  weeks) after STZ injections, the cortical expression of the following kinases was assessed by Western blot in 23-months old 3xTg-AD mice: **a**, phospho-ERK/total ERK ratio, **b**, total ERK, **c**, phospho-JNK/total JNK ratio, **d**, total JNK, **e**, GSK-3 $\beta$  phospho-S9/total GSK-3 $\beta$  ratio, **f**, total GSK-3 $\beta$ , **g**, phospho-CaMKII/total CaMKII ratio, **h**, total CaMKII, **i**, phospho-AKT/total AKT ratio, **j**, total AKT, **k**, p35, **l**, p25 and **m**, CDK5, and normalized to **n**,  $\beta$ -actin levels. Two representative lanes from each group of mice are displayed above the quantifications. Each individual in the data appears as a point on the graph. Data are presented as mean  $\pm$  SD and expressed as percentage of non-treated 23-months old 3xTg-AD mice (control group). Two-way ANOVAs were performed followed by Tukey's post hoc test. \* $p < 0.05$  vs. designated condition. CTL: non-treated control 3xTg-AD mice; STZ: 3xTg-AD mice subjected to STZ injections.

**Figure 4. Streptozotocin (STZ) administration led to impairments in the cortical activity of tau-related phosphatases in 23-months old 3xTg-AD mice.**

Three months ( $14 \pm 1$  weeks) after STZ injections, the cortical expression of the following phosphatases was assessed by Western blot in 23-months old 3xTg-AD mice: **a**, PP1, **b**, PP2A regulatory subunit A, **c**, PP2A-B $\alpha$  subunit, **d**, PP2A-B $\beta$  subunit, **e**, demethylated PP2A catalytic C subunit/total PP2A catalytic C subunit ratio, **f**, total PP2A catalytic C subunit, **g**, PP2B, and **h**, PP5, and normalized to  $\beta$ -actin levels. Two representative lanes from each group of mice are displayed above the quantifications. Each individual in the data appears as a point on the graph. Data are presented as mean  $\pm$  SD and expressed as percentage of non-treated 23-months old 3xTg-AD mice (control group). Two-way ANOVAs were performed followed by Tukey's post hoc test. \* $p < 0.05$ , and \*\* $p < 0.01$  vs. designated condition. CTL: non-treated control 3xTg-AD mice; STZ: 3xTg-AD mice subjected to STZ injections.

**Figure 5. Streptozotocin (STZ) administration induced an age-dependent exacerbation of cortical A $\beta$  accumulation in 3xTg-AD mice.**

Three months ( $14 \pm 1$  weeks) after STZ injections, the cortical levels of **a-c**, soluble A $\beta$ 40 and A $\beta$ 42 (pmol/g tissue), and **d-f**, insoluble A $\beta$ 40 and A $\beta$ 42 (pmol/g tissue), as well as the ratio of A $\beta$ 42/A $\beta$ 40, were assayed using ELISA. Each individual in the data appears as a point on the graph. Data are presented as mean  $\pm$  SD. Two-way ANOVAs were performed followed by Tukey's post hoc test. \* $p < 0.05$  vs. designated condition. CTL: non-treated control 3xTg-AD mice; STZ: 3xTg-AD mice subjected to STZ injections.

**Figure 6. Streptozotocin (STZ) administration did not result in an exacerbation of cortical synaptic deficits in 3xTg-AD mice.**

Three months ( $14 \pm 1$  weeks) after STZ injections, the cortical expression of the following synaptic markers was assessed by Western blot: **a**, Drebrin, **b**, PSD95, **c**, Synaptophysin, and **d**, SNAP-25, and normalized to  $\beta$ -actin levels. Two representative lanes from each group of mice are displayed above the quantifications. Each individual in the data appears as a point on the graph. Data are presented as mean  $\pm$  SD and expressed as percentage of non-treated 7-months old 3xTg-AD mice (control group). Two-way ANOVAs were performed followed by Tukey's post hoc test. \* $p < 0.05$ , \*\* $p < 0.01$  and \*\*\* $p < 0.001$  vs. designated condition. CTL: non-treated control 3xTg-AD mice; STZ: 3xTg-AD mice subjected to STZ injections.

**Figure 7. Streptozotocin (STZ) administration led to an age-dependent impairment in cortical insulin signaling in 3xTg-AD mice.**

Three months ( $14 \pm 1$  weeks) after STZ injections, the cortical expression of the following markers associated with insulin signaling was assessed by Western blot: **a**, phospho-IR (Insulin Receptor)/total IR ratio, **b**, total IR, **c**, phospho-PI3K/total PI3K ratio, **d**, total PI3K, and **e**, IDE (Insulin Degrading Enzyme), and normalized to  $\beta$ -actin levels. Two representative lanes from each group of mice are displayed above the quantifications. Each individual in the data appears as a point on the graph. Data are presented as mean  $\pm$  SD and expressed as percentage of non-treated 7-months old 3xTg-AD mice (control group). Two-way ANOVAs were performed followed by Tukey's post hoc test. \* $p < 0.05$ , \*\* $p < 0.01$  and \*\*\* $p < 0.001$  vs. designated condition. CTL: non-treated control 3xTg-AD mice; STZ: 3xTg-AD mice subjected to STZ injections.

**Figure 8. Age-dependent decline in blood-brain-barrier (BBB) integrity in 3xTg-AD mice.**

Three months ( $14 \pm 1$  weeks) after STZ injections, the cortical expression of the following markers related to BBB integrity was assessed by Western blot: **a**, ZO1, **b**, Occludin, and **c**, VE-

Cadherin, and normalized to  $\beta$ -actin levels. Two representative lanes from each group of mice are displayed above the quantifications. Each individual in the data appears as a point on the graph. Data are presented as mean  $\pm$  SD and expressed as percentage of non-treated 7-months old 3xTg-AD mice (control group). Two-way ANOVAs were performed followed by Tukey's post hoc test. \* $p < 0.05$ , \*\* $p < 0.01$  and \*\*\* $p < 0.001$  vs. designated condition. CTL: non-treated control 3xTg-AD mice; STZ: 3xTg-AD mice subjected to STZ injections.

Journal Pre-proof

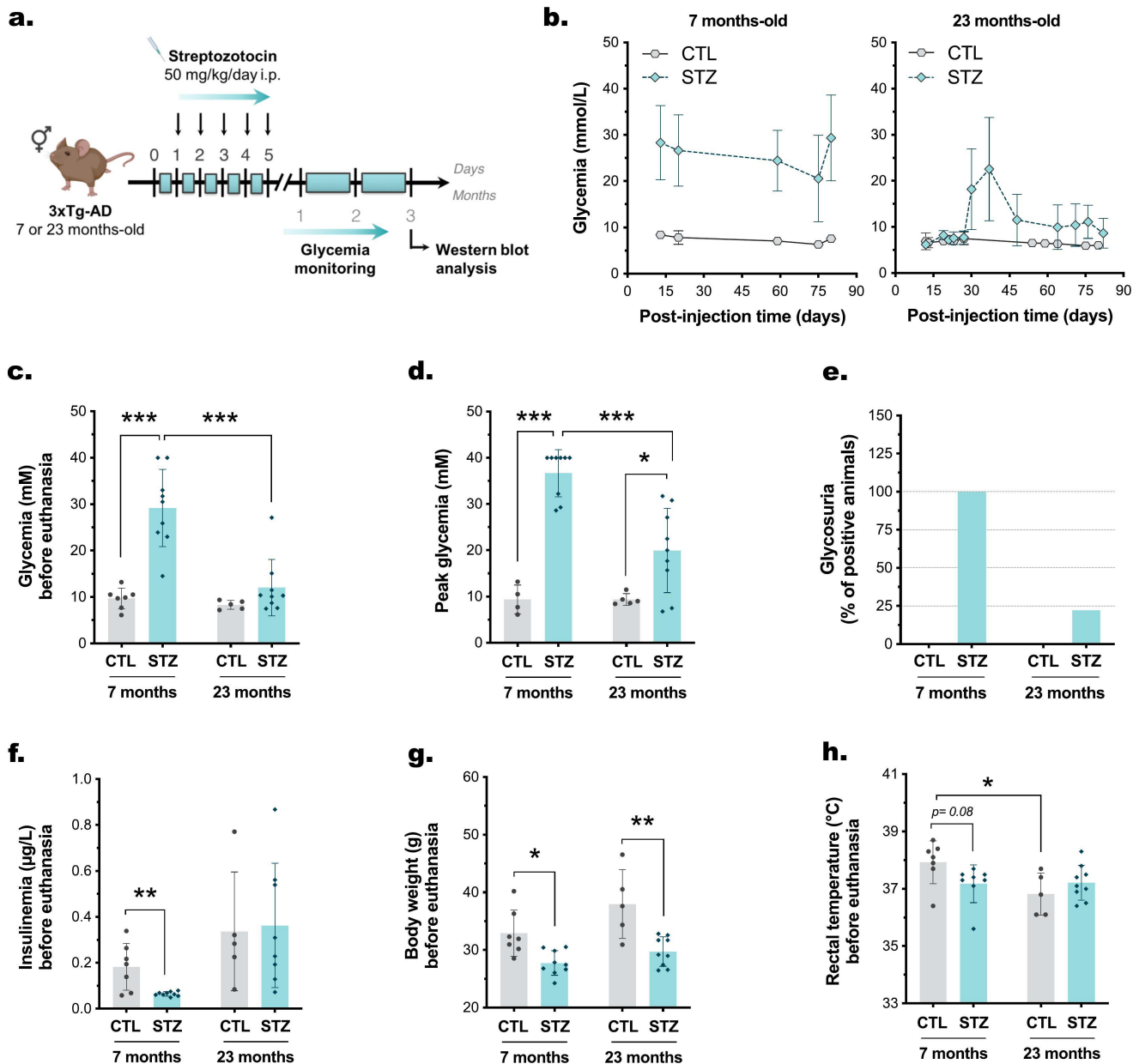


Figure 1

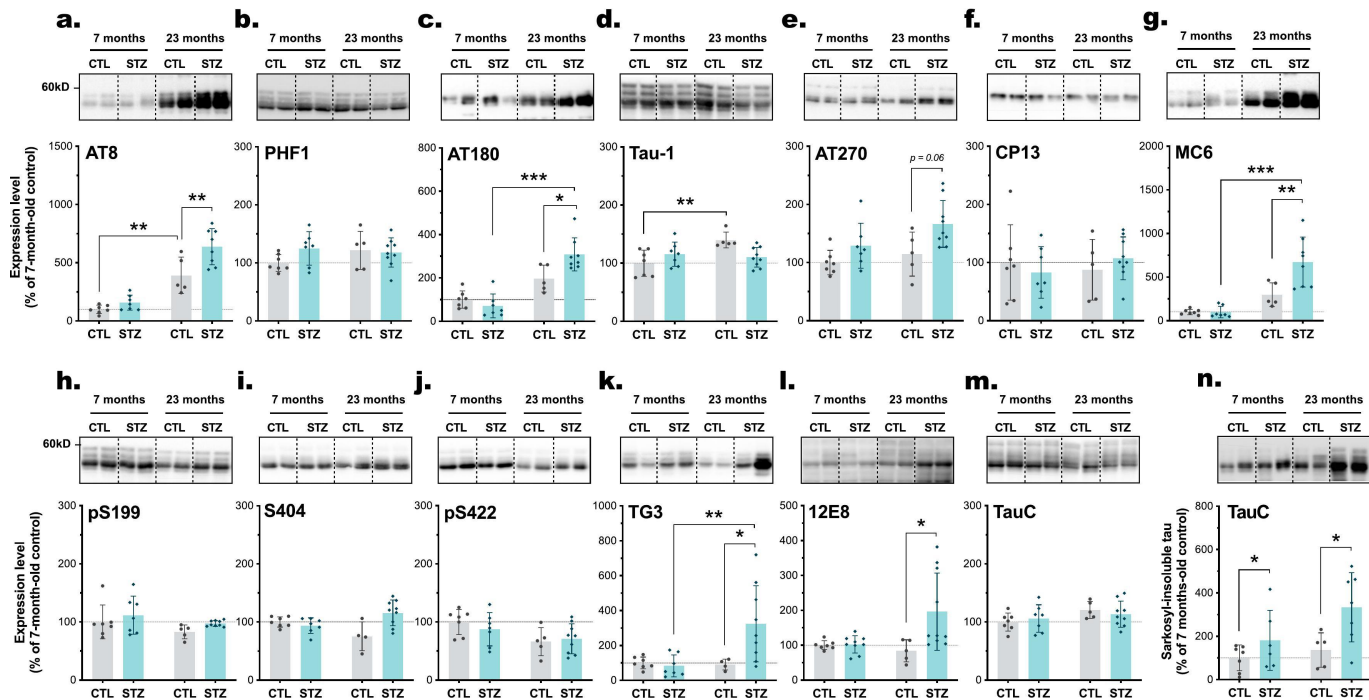


Figure 2

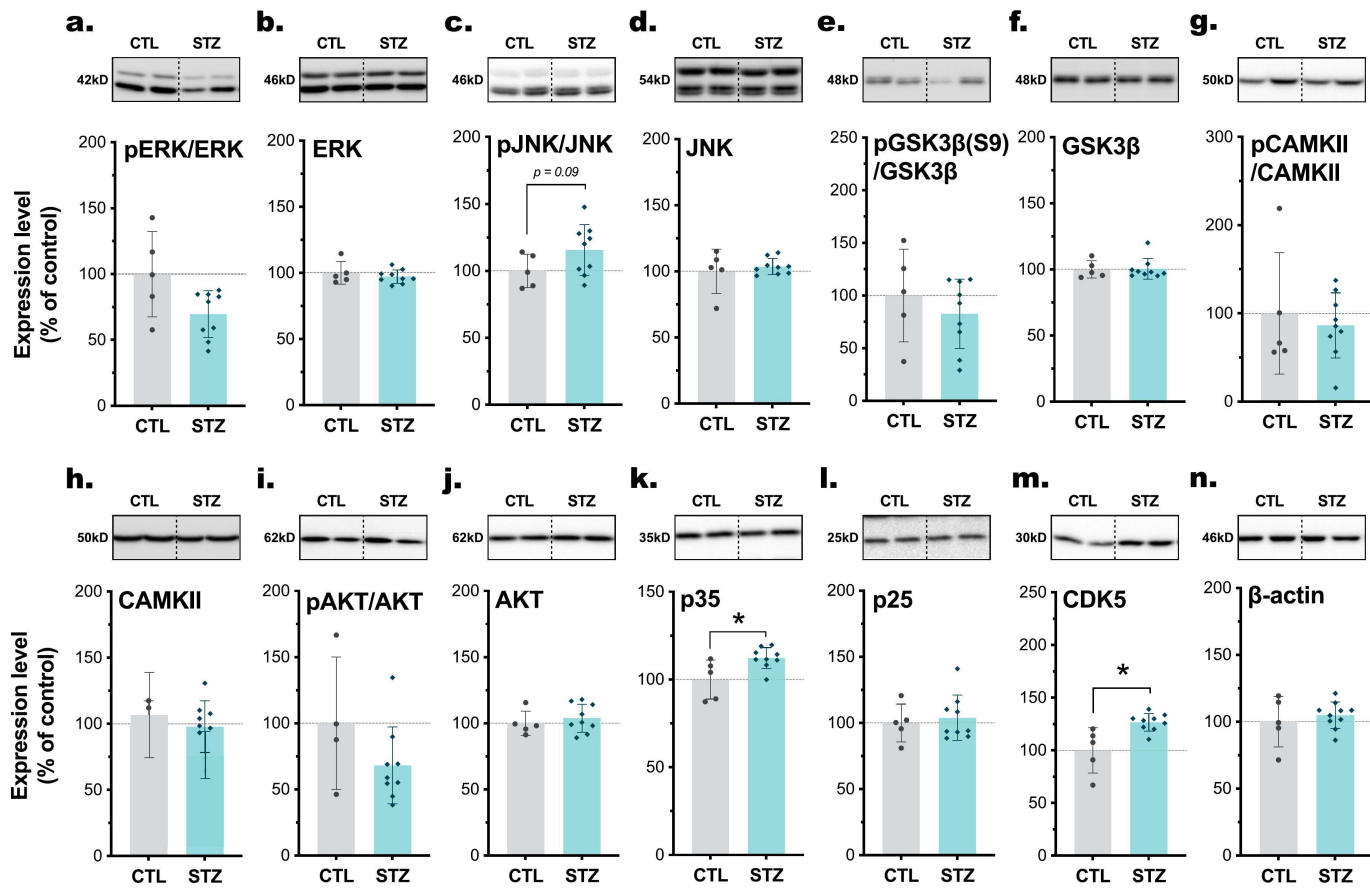


Figure 3

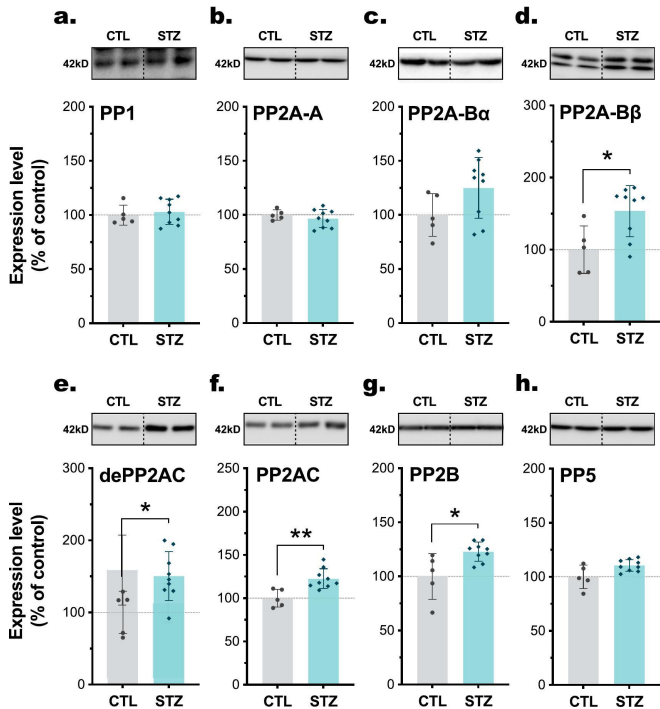


Figure 4

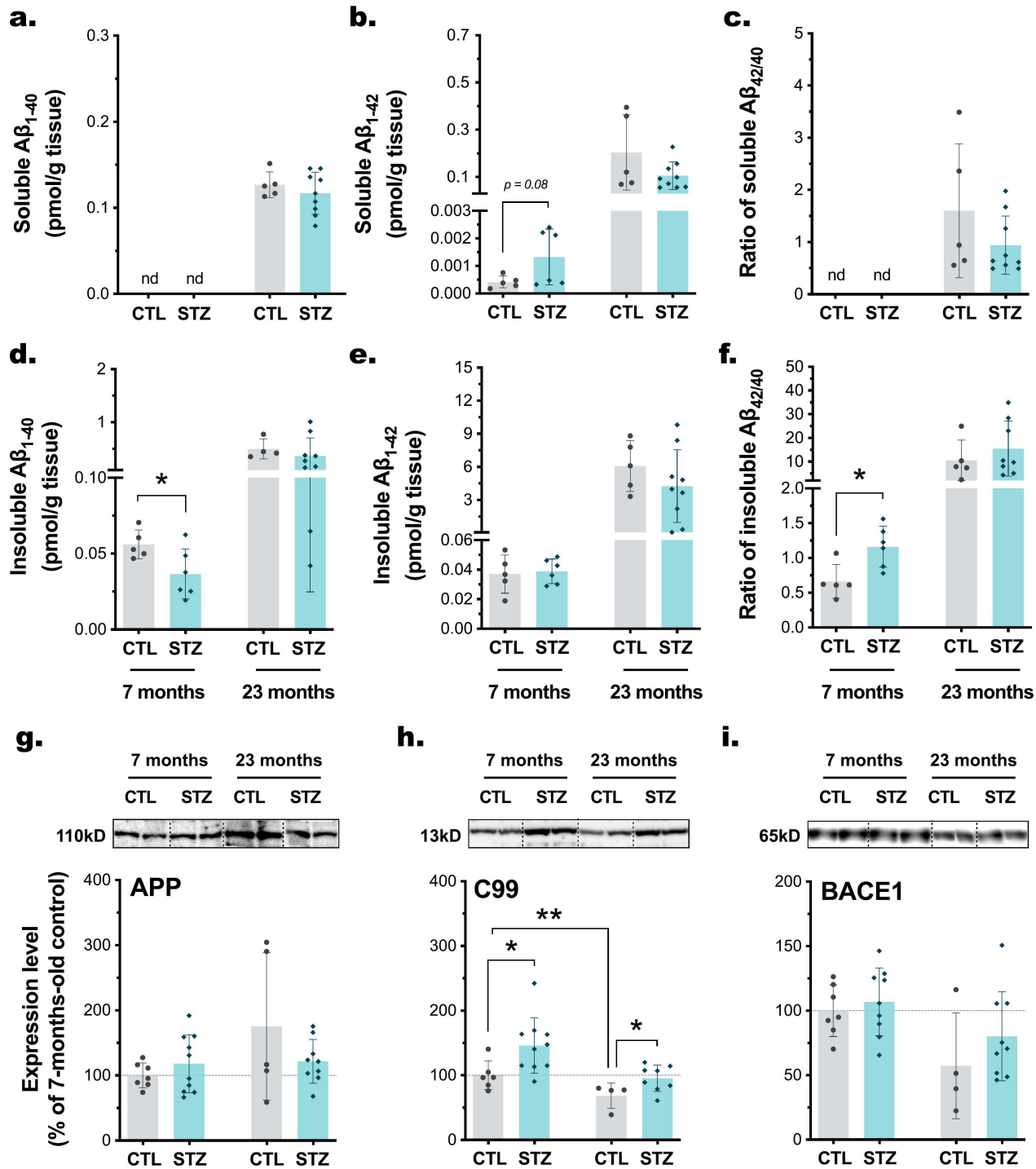


Figure 5

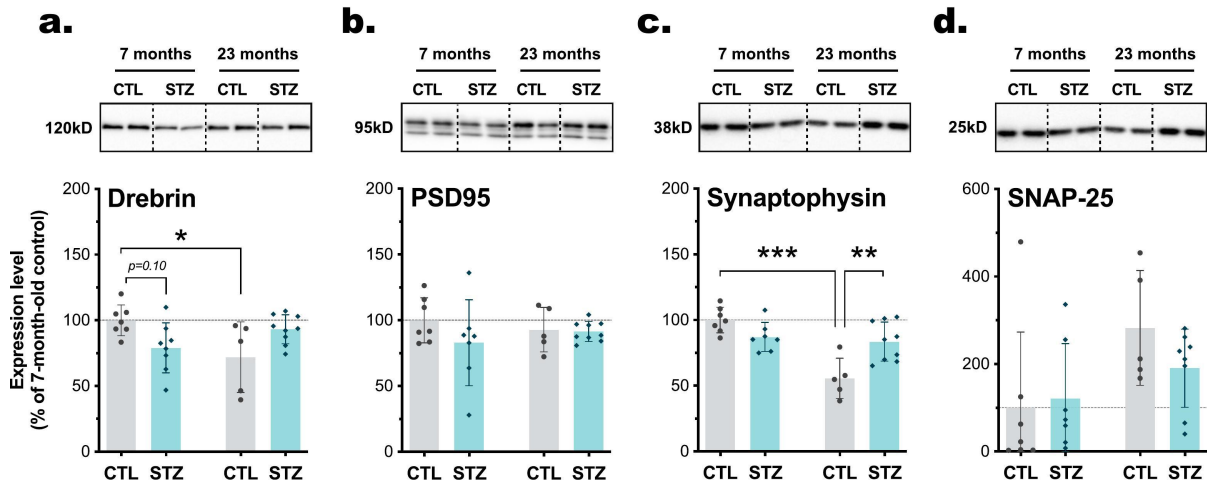


Figure 6

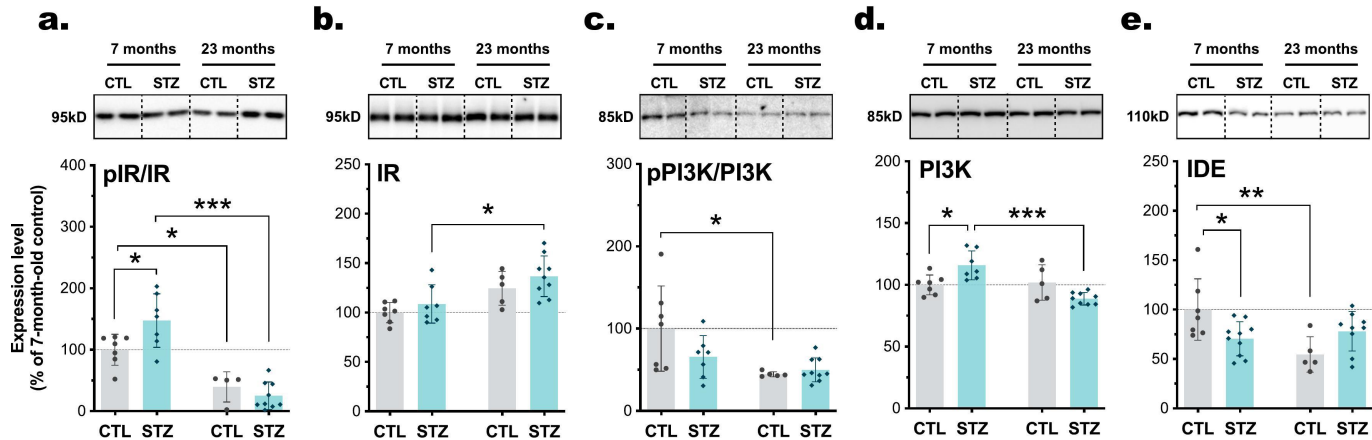


Figure 7

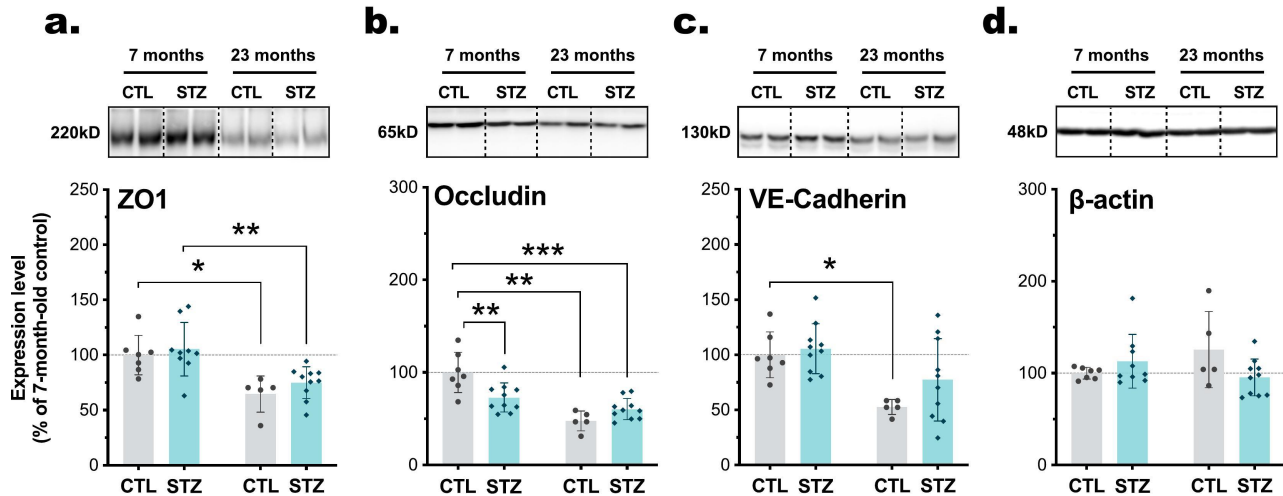


Figure 8